Development of Land Surface Elevation Adjustment Due to Subsidence in the Spring Creek and Willow Creek Watersheds Based on Measured Historical and Simulated Future Subsidence Rates

Prepared for:

Harris-Galveston Subsidence District
1660 W Bay Area Blvd
Friendswood, TX, 77546
(281) 486-1105

Prepared by:

INTERA Incorporated
Three Sugar Creek Center Blvd
Suite 675
Sugar Land, TX 77478
(832) 535-5763

Originally Released: October 2021
Revised Title for Clarity: November 2022

This page is intentionally left blank.

PROFESSIONAL GEOSCIENTIST SEAL

The work shown in the following document was overseen by the following Licensed Professional Geoscientist:

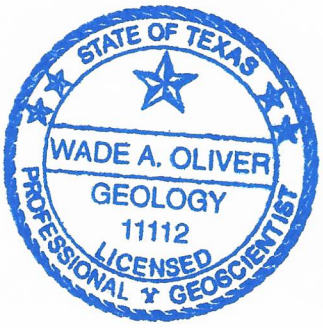

Wade A. Oliver, Texas Licensed Professional Geoscientist #11112

11/9/2022

Date

Firm PG License No. 50189

This page is intentionally left blank.

TABLE OF CONTENTS

LIST OF FIGURES

ACROYNMS AND ABBREVIATIONS

CGWU	Current Groundwater Use
FBSD	Fort Bend Subsidence District
GPS	Global Positioning System
HAGM	Houston Area Groundwater Model
HGSD	Harris-Galveston Subsidence District
InSAR	Interferometric Synthetic Aperture Radar
LGWU	Limited Groundwater Use
LSGCD	Lone Star Groundwater Conservation District
SAR	Synthetic Aperture Radar
SJRA	San Jacinto River Authority
SMU	Southern Methodist University
TxDOT	Texas Department of Transportation
USGS	United States Geological Survey

This page is intentionally left blank.

1.0 INTRODUCTION

The Harris-Galveston Subsidence District ("HGSD") selected consultants (Michael Baker International, LLC, ["Michael Baker"] and INTERA Incorporated ["INTERA"]) to evaluate subsidence impacts on flood risk within the Spring Creek and Willow Creek watersheds (**Figure 1-1**). INTERA was tasked with the development of current and future subsidence grids that will be used to modify elevations in the hydrologic and hydraulic modeling employed by Michael Baker.

To evaluate the effects of changing groundwater pumping on subsidence, INTERA developed subsidence grids for two scenarios that reflect different rates of subsidence in the areas of Montgomery County that can receive treated surface water. The two scenarios are:

> **Limited Groundwater Use (LGWU) Scenario** – Beginning in 2016, groundwater use in Montgomery County was limited to approximately 64,000 acre-feet per year in response to regulations imposed by the Lone Star Groundwater Conservation District ("LSGCD"). This represented an approximately 30 percent reduction in groundwater usage county-wide. The blue hashed region in **Figure 1-1** represents the area that reduced groundwater usage and began receiving treated surface water from the San Jacinto River Authority ("SJRA"). The reduced groundwater withdrawals decreased subsidence rates measured at global positioning system ("GPS") stations and by remote sensing techniques, such as Interferometric Synthetic Aperture Radar (InSAR), in and near the SJRA service area. The LGWU scenario incorporates the reduced subsidence rates in these areas resulting from the reductions in groundwater use and assumes these rates continue through 2070.
>
> **Current Groundwater Use (CGWU) Scenario** – The CGWU scenario represents subsidence rates that pre-date groundwater reductions in 2016 and applies these rates through 2070.

Both scenarios consider the expected slowing of subsidence resulting from planned conversions in Regulatory Area 3 in northern Harris County based on the HGSD Regulatory Plan. The plan requires that all water users reduce reliance on groundwater to no more than 40 percent of total water demand by 2025 and to no more than 20 percent of total water demand by 2035. The groundwater conversions in Harris County were incorporated into the two scenarios using modeled values from the Houston Area Groundwater Model ("HAGM"; Kasmarek, 2013).

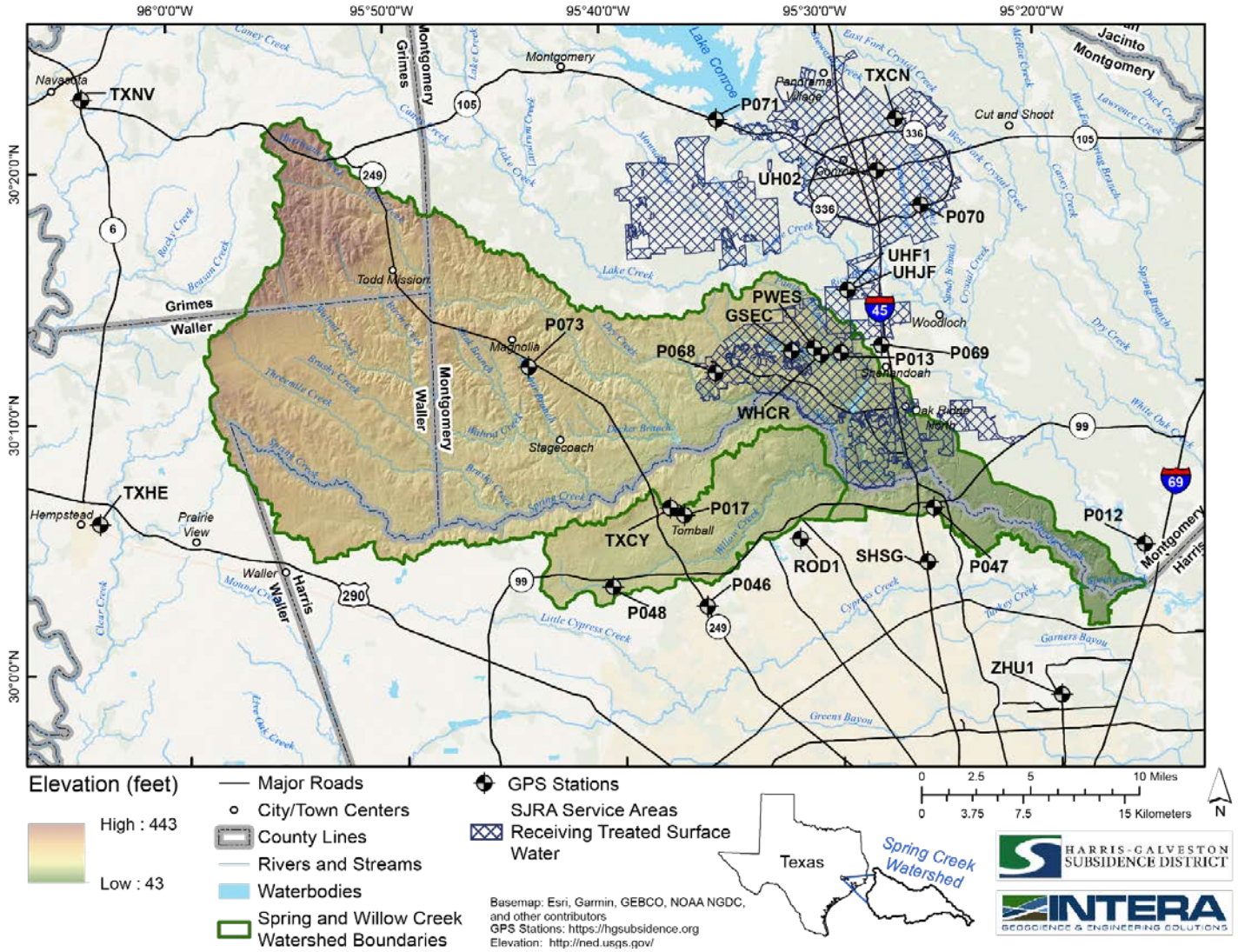

Figure 1-1 Spring and Willow Creek watersheds with the 24 GPS stations used in the study and the San Jacinto River Authority (SJRA) service areas provided with surface water.

2.0 SUBSIDENCE DATA SOURCES

This study uses subsidence observations from GPS stations and InSAR datasets, which together provide the spatial and temporal subsidence rate and magnitude data needed for the subsidence projections. Over the past two-decades, the Districts (HGSD and the Fort Bend Subsidence District ["FBSD"]), in cooperation with the Brazoria County Groundwater Conservation District, the Lone Star Groundwater Conservation District, the University of Houston, the Texas Department of Transportation ("TxDOT") and other cooperating entities have operated a network of approximately 200 GPS stations monitoring vertical and lateral changes of the land surface. Southern Methodist University ("SMU") also uses available Synthetic Aperture Radar ("SAR") datasets to study spatial trends in land surface deformation throughout the greater Houston area. The SAR interferometry technique uses two SAR images of the same area acquired at different times and "interferes" (differences) them, resulting in maps called interferograms that show ground-surface displacement (range change) between the two time periods (Solt and Sneed, 2014). The strategy used to develop the subsidence grids, which is detailed below, was developed to utilize the high temporal resolution of the GPS data, the high spatial resolution of SAR data, and model/literature estimates when and where observed data were not available.

2.1 GPS Monitoring Stations

There are 10 GPS stations that lie within the Spring and Willow Creek watersheds. These GPS stations measure both vertical and horizontal movement of the land surface. Because the focus of our analysis is on how the GPS data inform subsidence rates, only data on vertical movement in land surface (i.e., elevation) were used. A negative displacement measured at a GPS station indicates subsidence while a positive displacement indicates uplift.

Subsidence rate data from the 10 GPS stations within the study area and an additional 14 GPS stations located in the surrounding area were analyzed (**Figure 1-1**). If available, subsidence rate data from before 2016 were fit with a linear regression to estimate subsidence rates prior to the reduction in groundwater use in Montgomery County. Subsidence rate data collected after 2016 were also fit with linear regressions to estimate the change in subsidence rates. **Figure 2-1** shows the data from GPS station P013 and a linear regression of the rate of subsidence before and after 2016. For this location, the CGWU subsidence rate was calculated to be -0.71 inches per year and the LGWU subsidence rate is calculated to be -0.17 inches per year (see **Figure 2-1**). Similar figures were developed for the remaining 23 GPS stations analyzed and are included in **Appendix A.**

2.2 InSAR-derived Data

InSAR techniques can measure ground surface deformation at high spatial resolutions over large areas (Qu and others, 2015; Qu and others 2019). SMU provided two ground surface deformation datasets that were developed using SAR datasets. The two SAR datasets provide average subsidence rates. The average subsidence rates are calculated over two time periods: 2007-2011 and 2016-2020. The 2007-2011 average subsidence rate data were derived from measurements made by the ALOS-1 satellite and are used in this analysis to inform the spatial distribution of subsidence rates expected in the CGWU scenario. The 2016-

2020 dataset was derived from the Sentinel-1A/B satellite (S1A) and is used to define the spatial distribution of subsidence rates in the LGWU scenario.

Figure 2-2 shows the ALOS-1 InSAR-derived deformation data, which are not spatially continuous over the Spring Creek watershed. Because spatially continuous data is needed for subsidence grid development, the ALOS-1 InSAR-derived data was interpolated using a common interpolation technique known as kriging. A key step in processing SAR data is georeferencing, which is used to tie InSAR-derived deformation rates to measurements made on the ground surface. To georeference the SAR data, InSAR-derived estimates of displacement are correlated with GPS measured subsidence values and then normalized. This process puts the SAR data into absolute elevation framework. The ALOS-1 data were georeferenced to the ground surface using GPS station data (see Qu and others, 2015).

Figure 2-3 shows the S1A InSAR-derived subsidence rate data, which are nearly continuous over the watershed. The few cells without data were assigned values using an average of the neighboring cells. The S1A InSAR-derived data were preliminary when we received them and had not yet been georeferenced. However, because we are only concerned with changes in the relative rates of subsidence between the two periods (2007-2011 and 2016-2020) the georeferencing step is not needed.

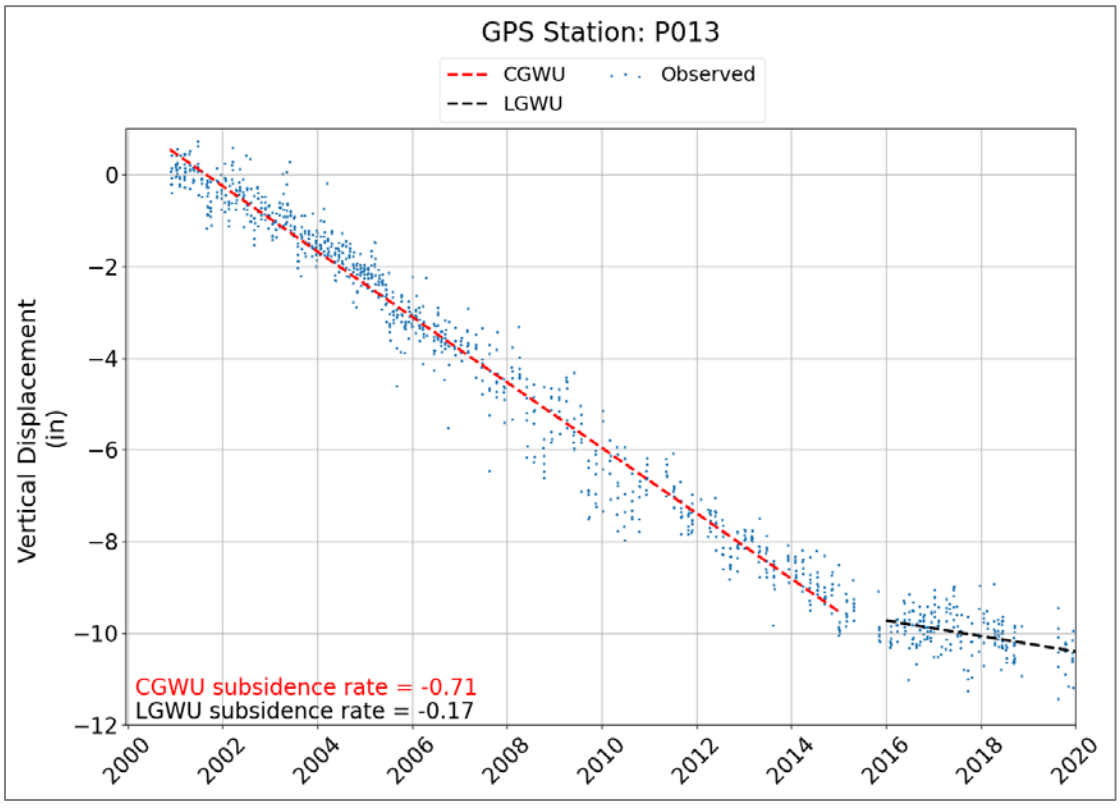

Figure 2-1 Observed vertical displacement at P013 GPS station. Negative values indicate subsidence.

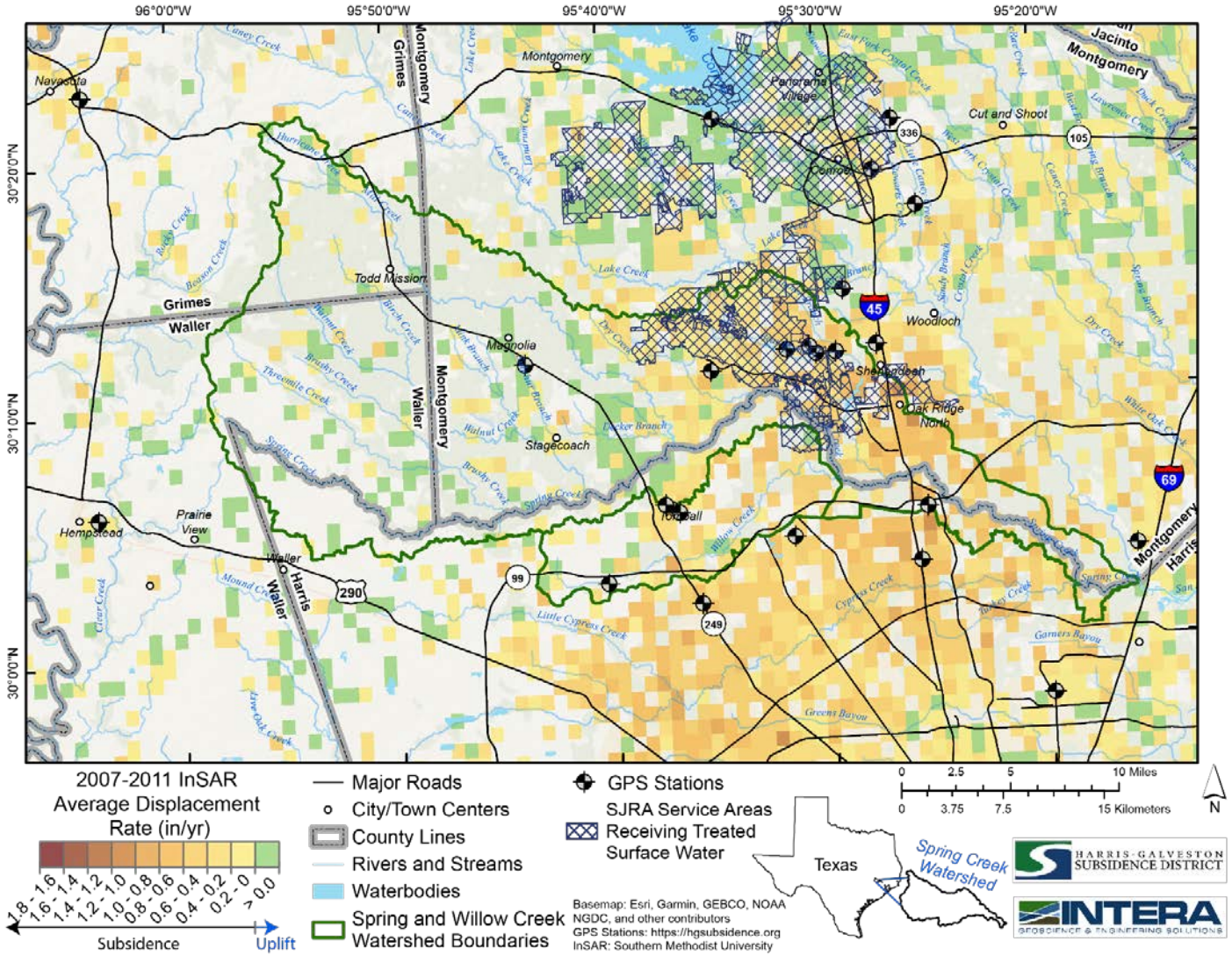

Figure 2-2 Average subsidence rates from 2007 to 2011 in the InSAR data from the ALOS satellite

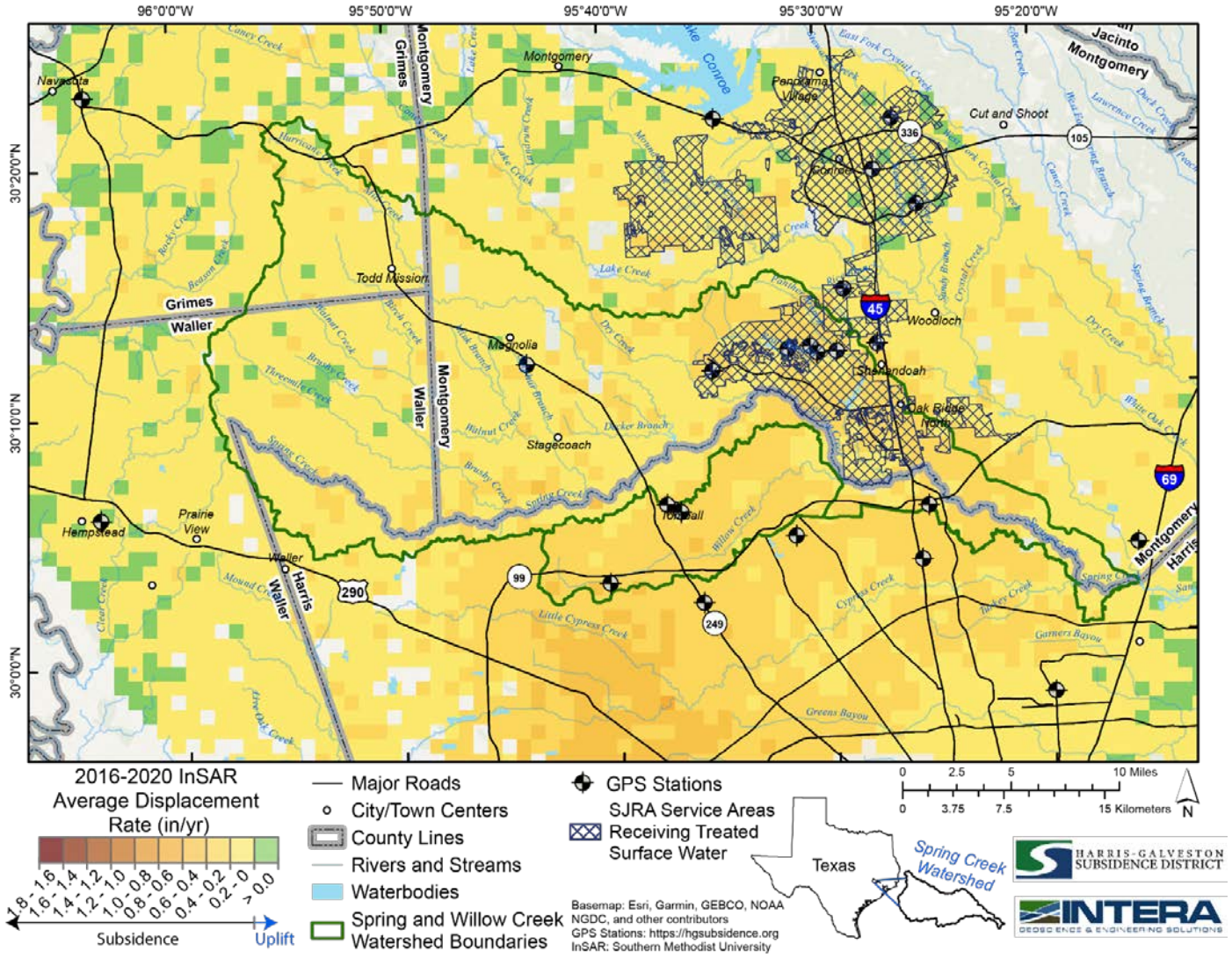

Figure 2-3 Average subsidence rates from 2016 to 2020 in the InSAR data from the S1A satellite.

2.3 Houston Area Groundwater Model

To incorporate the change in subsidence resulting from HGSD 2013 Regulatory Plan conversions in 2025 and 2035, the Houston Area Groundwater Model ("HAGM") was used to define subsidence rates in the portion of the watersheds that lie within Harris County. The HAGM was developed by the United States Geological Survey ("USGS") to simulate groundwater flow and land surface subsidence in the northern portion of the Gulf Coast Aquifer System from predevelopment (defined as 1891 in the model) through 2009 (Kasmarek and others, 2004; Kasmarek and others, 2013). During the development of the 2013 Regulatory Plan, the HAGM was used as a tool to predict future subsidence. The subsidence predictions in the model were used to define subsidence rates in Harris County between 2025 and 2070.

2.4 Natural Subsidence

Subsidence can be caused by both natural and anthropogenic processes. Natural processes, which occur on geologic timescales (over 100,000 years), are driven by natural overburden pressures that cause gradual compaction of underlying fine-grained interbeds. Rates associated with this natural consolidation in the coastal region of Texas can be less than 0.01 inches per year (Morton, 1979; Winker, 1979; and Paine, 1991), but can vary depending on properties of the underlying unconsolidated aquifers. In contrast, subsidence on more recent time scales and influenced by anthropogenic activities can be significantly larger as shown in **Figure 2-1**. In areas where natural subsidence is occurring and measured, long-term projections of subsidence can incorporate both natural rates of subsidence (considered to be constant over long time periods) and anthropogenic rates of subsidence, which can change rapidly in response to changes in groundwater use.

Using GPS data and multidecadal to century tide gauge data, Zhou et al. (2021) estimated that natural subsidence rates along the Texas coastline are on average 0.064 inches per year. This estimate was incorporated in both subsidence grid scenarios as a baseline value. That is, nowhere in the grid is the subsidence rate less than 0.064 inches per year. Zhou et al. (2021) indicated that natural subsidence along the Texas coast varies between 0.02 inches per year and 0.14 inches per year. They suggest that this variability is driven by differences in thickness of the unconsolidated aquifers, which generally thin with increasing distance from the coast. Increased aquifer thickness suggests that more unconsolidated units could be present and the effective stress, which drives compaction, on those units is greater given the increased overburden pressure. Zhou et al. (2021) noted that the thickness of the Jasper aquifer is one of the key drivers of variation in natural subsidence because its thickness ranges from less than 50 feet in thin outcrop areas to more than 5,000 feet closer to the coast. Given the inland location of Spring and Willow Creek watersheds and an average Jasper aquifer thickness of 1060 feet within the watersheds, we conclude the average natural subsidence rate of 0.064 inches per year is appropriate.

3.0 APPROACH USED TO DEVELOP ANNUAL SUBSIDENCE ESTIMATES

Given the different characteristics of the subsidence data introduced above, INTERA developed a strategy that utilizes the strengths of each data source. The data were used to inform subsidence rates on a network of points that were evenly spaced (1 point for every 9 km^2) over a region that includes the study watershed and a 4.8-km zone that surrounds the study watershed (**Figure 3-1**). These points were interpolated to create a smooth distribution of subsidence rates that accounts for the fact that impacts from changes in groundwater use do not abruptly change at county lines or along the area where SJRA can deliver surface water. In **Figure 3-1,** annual subsidence rates at the orange circles were estimated using the InSAR and GPS data prior to the planned Harris County conversions in 2025 and post-2025 were estimated using the HAGM predicted rates. Outside of Harris County, the GPS station data were used to inform the magnitudes of subsidence, while the InSAR data was used to define the spatial distribution. The integration of these two sources of data was achieved by investigating the relationship between the GPS data and InSAR data. The method used to inform subsidence at these points is outlined in **Figure 3-2** and each step is discussed below.

The first step in the process required normalizing (on a scale of 0 to 1) the CWGU InSAR data and the LGWU InSAR data (**Figures 2-2** and **2-3**), where zero indicates little to no subsidence and one indicates the highest rate of subsidence (**Figures 3-3 and 3-4**). The InSAR datasets were normalized because the LGWU InSAR dataset was not georeferenced so only relative changes could be evaluated.

In step two, the linear regression approximated GPS subsidence rate data for the CWGU and LWGU scenarios were interpolated onto a grid of cells using an inverse distance weighting technique (**Figures 3-5 and 3-6**). Because of the limited number of GPS data (17 stations with pre-2016 data that apply to the CGWU scenario and 24 stations with post-2016 data that apply to the LGWU scenario) and the lack of GPS data in some areas (e.g., the western part of the study watershed), there is inherent uncertainty associated with these two surfaces. There may also be spatial biases driven by differences in land use and the location of most GPS stations within urban environments. For example, in the western portion of the watershed, three GPS stations located in urban environments inform the distribution of subsidence rates in a region that is more rural (area between Magnolia and Navasota).

In step there, the relations between the normalized InSAR surfaces and the interpolated GPS surfaces were established by sampling each surface using a grid of sample points spaced every 1 km by 1 km (**Figure 3-2**). The sampled InSAR surface values and the sampled GPS surface values for both the CGWU and LGWU scenarios were plotted as boxplots in step four. In step four of **Figure 3-2,** the blue boxes show the quartiles of each data bin while the whiskers (grey) extend to show the rest of the distribution except for data points that are determined to be outliers. The median of each data bin is shown as a horizontal black line. The general trends in the boxplots are as expected. That is, as normalized InSAR values increase, subsidence rates from the GPS station surfaces also increase (i.e., vertical displacements rates become more negative).

The median GPS values from the boxplots were plotted against the normalized InSAR values in step five. Normalized InSAR values less than 0.3 were removed because these data corresponded with areas in the GPS interpolated surfaces which are considered of higher relative uncertainty such as the western part of the watershed where there was minimal GPS data informing the distribution. Linear regressions were used to approximate the relationship between the median GPS values and the normalized InSAR values.

To address the lack of GPS data in the lower range of the normalized InSAR values, the y-intercept was fixed to 0.064 inches per year, which is the average natural subsidence rate for the Texas costal region estimated by Zhou et al. (2021). While there is uncertainty in the actual natural subsidence rate, it appears significantly lower in magnitude than the LGWU subsidence rate in 23 of 24 GPS stations (**Appendix A**). Because the hydrologic and hydraulic modeling will be a comparison between two subsidence scenarios which consider the same natural subsidence rate, the effects of the actual natural subsidence rate on study conclusions should be neutral.

In step six, the linear regressions from step five are used to create annual subsidence grids. The values from the normalized InSAR surfaces are multiplied by the calculated slope and then the y-intercept is subtracted, yielding annual subsidence values that are informed by both InSAR and GPS station subsidence rate data.

For each year between 2018 and 2070, the subsidence surface values are sampled to the network of points shown in **Figure 3-1**. After the 2025 and 2035 conversions, the HAGM subsidence estimates in some areas were below the natural subsidence rate suggested for the region (0.064 inches per year). To address this issue, a baseline value of 0.064 inches per year was enforced. Another important consideration is that in a review of the 2013 Regulatory Plan, INTERA found that the HAGM appears to underestimate subsidence in northern Harris County. A portion of this area lies within the study watershed, and thus underestimated model subsidence rates translate to lower projected total subsidence in the subsidence grids. The final subsidence grid for each year was determined by interpolating over the network of points shown in **Figure 3-1** using an inverse distance weighting technique.

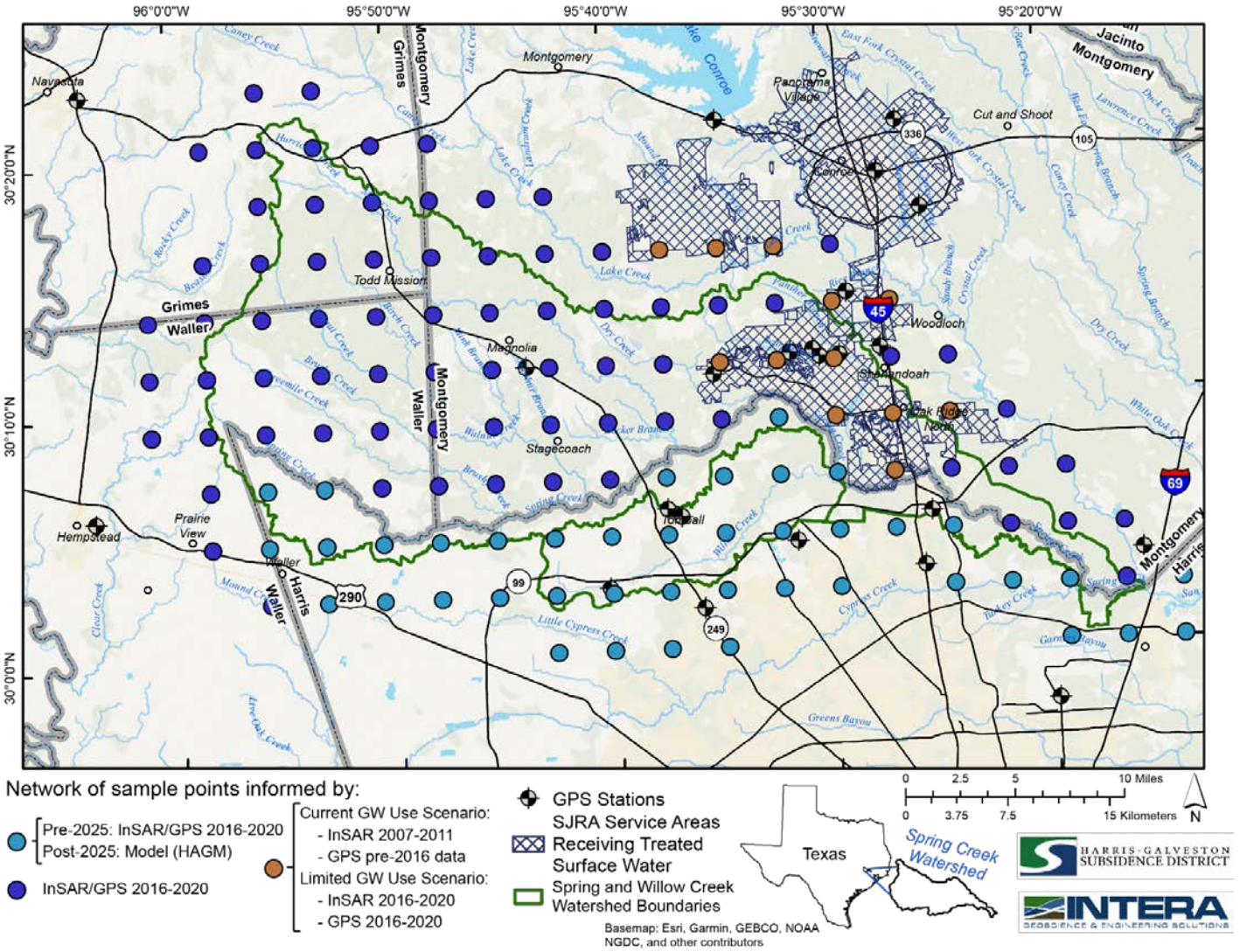

Figure 3-1 Network of samples points where subsidence rates are estimated and interpolated.

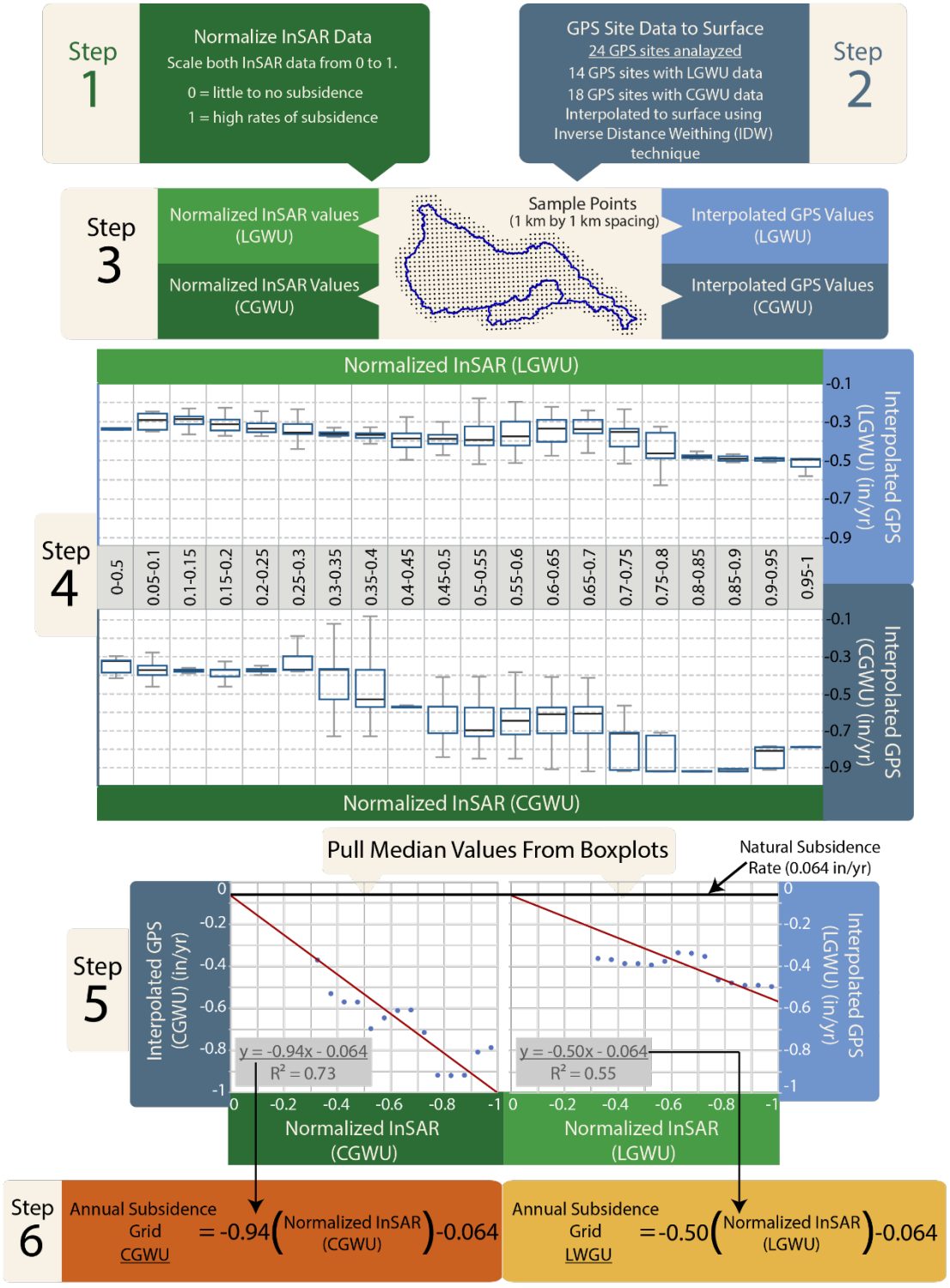

Figure 3-2 Flowchart outlining the procedure used to create the annual subsidence grids

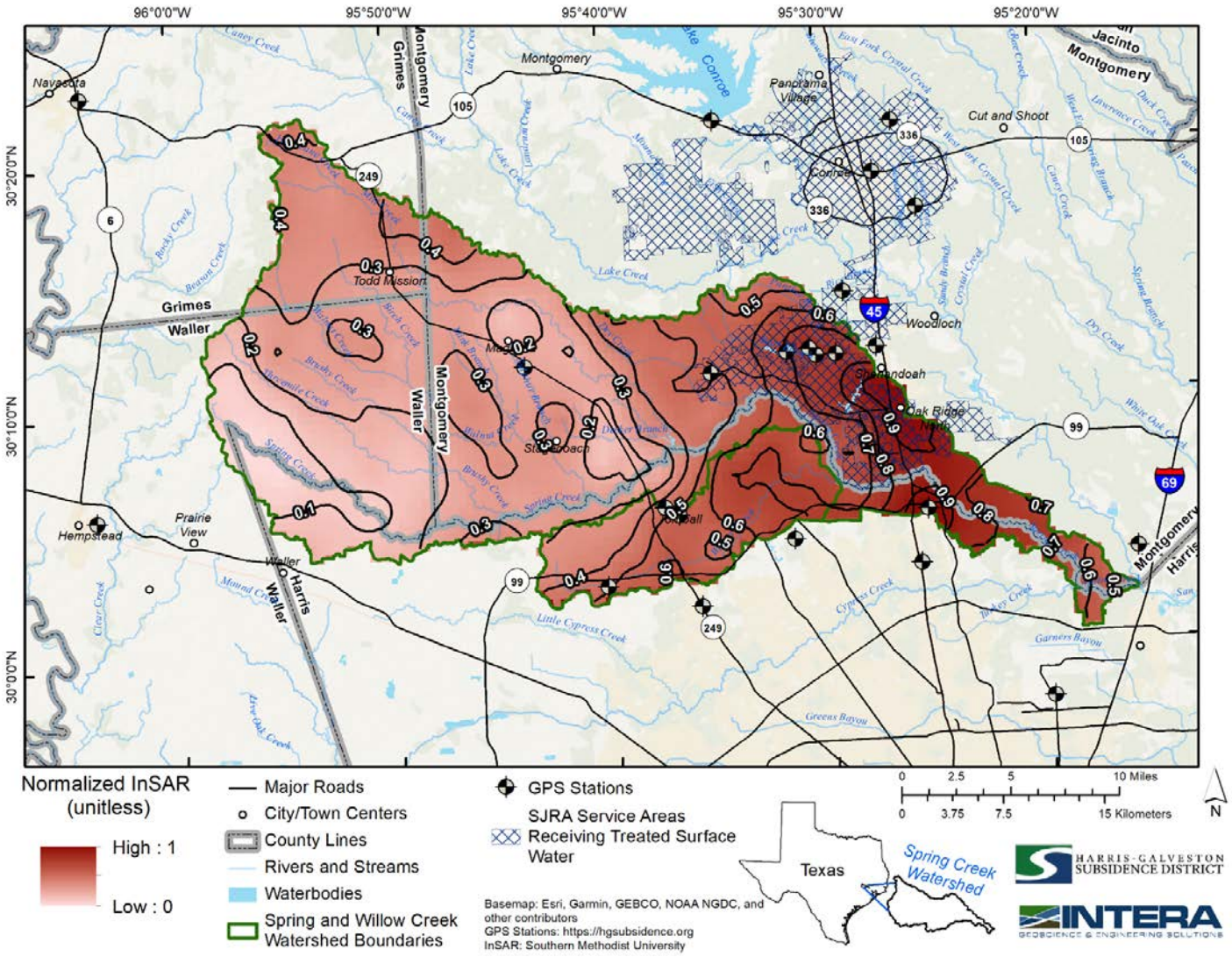

Figure 3-3 Normalized InSAR-derived subsidence rates from 2007 to 2011

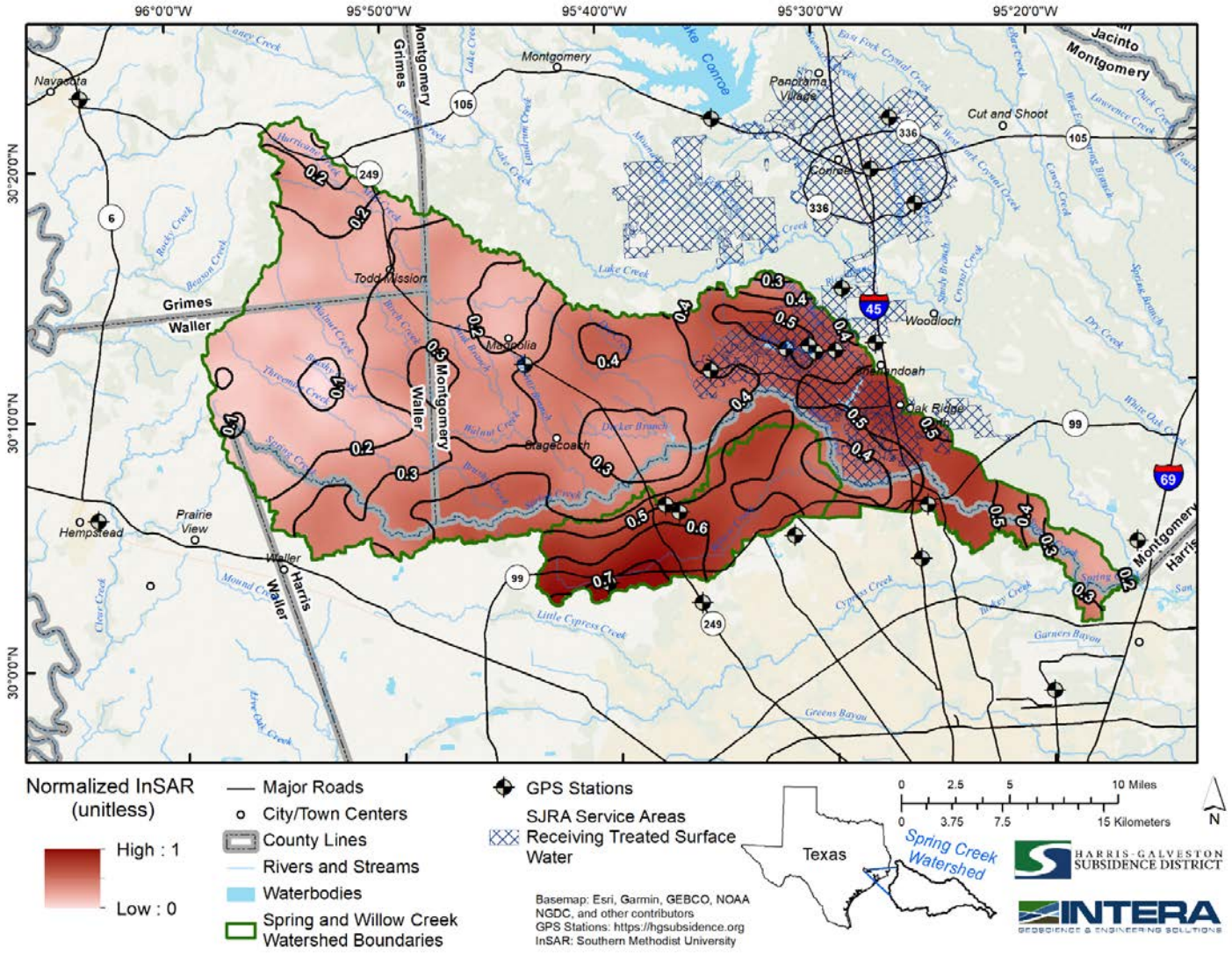

Figure 3-4 Normalized InSAR-derived subsidence rates from 2016 to 2020

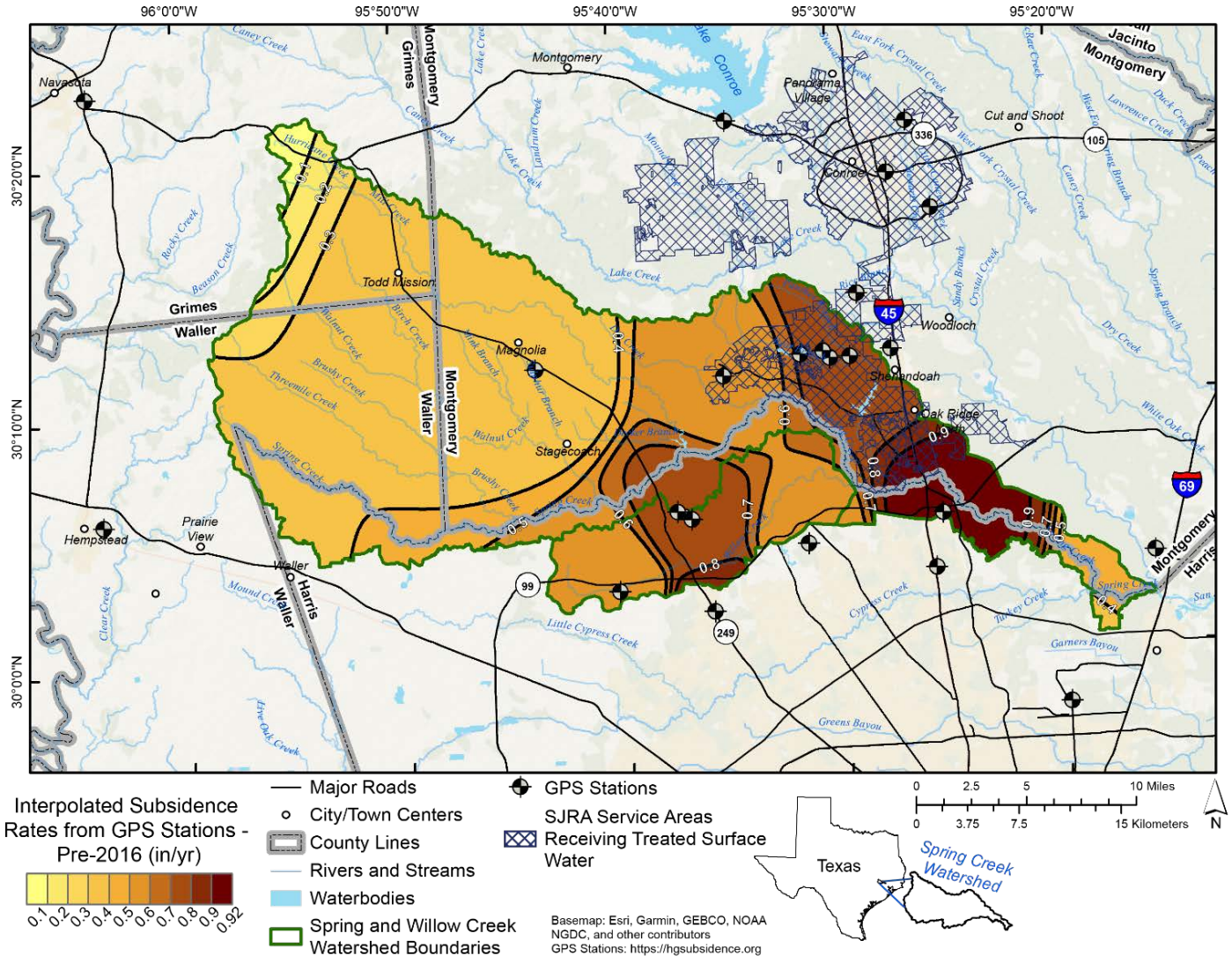

Figure 3-5 Interpolation of GPS station subsidence rates prior to 2016

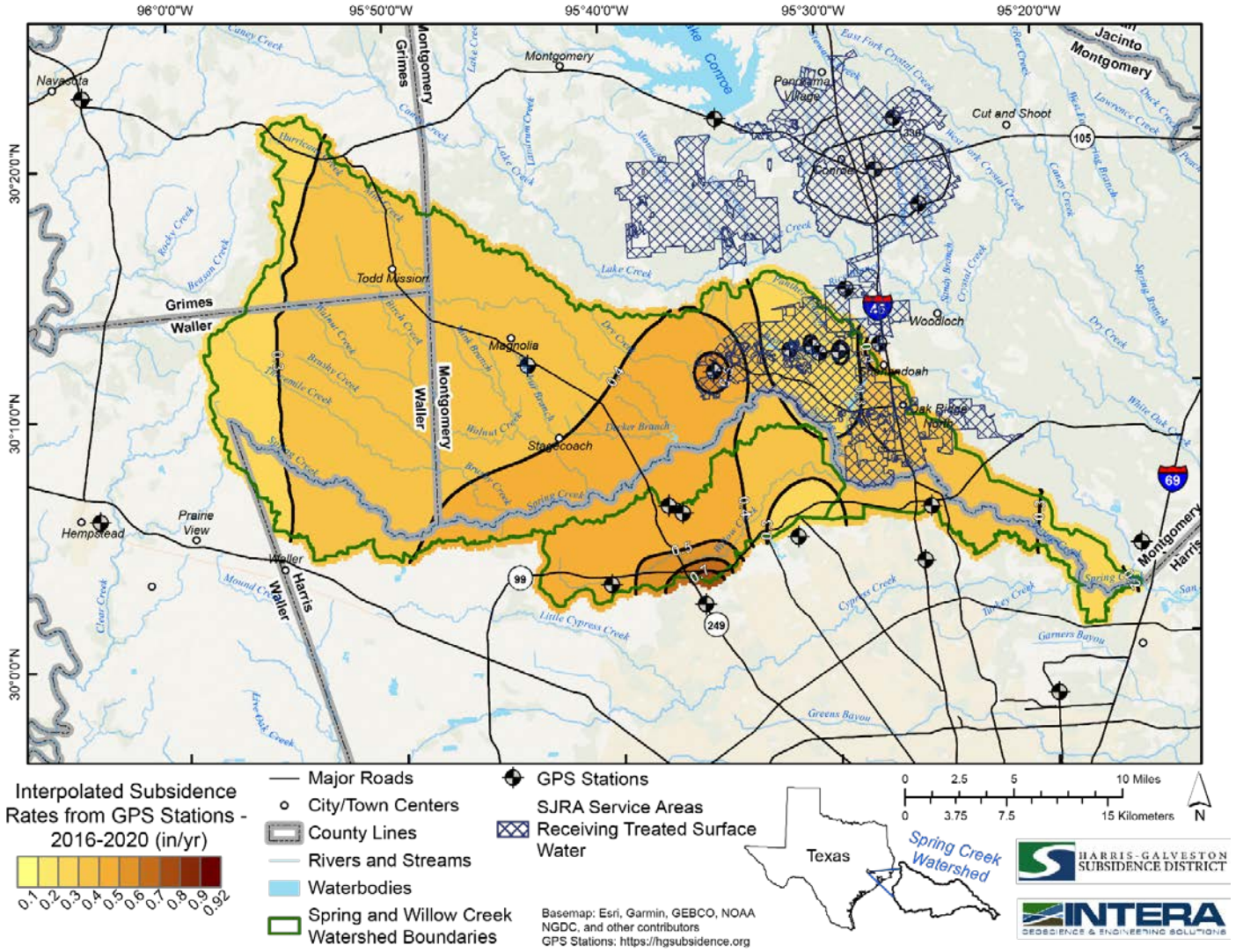

Figure 3-6 Interpolation of GPS station subsidence rates from 2016 to 2020

4.0 SUBSIDENCE PROJECTIONS

The total subsidence between 2018 and 2070 was calculated for both scenarios by adding the 52 interpolated subsidence surfaces calculated over that period (**Figures 4-1 and 4-2**). Differences of 0.2 to 1.25 feet in total subsidence between the LGWU and CGWU scenario are observed within and near the SJRA services areas receiving treated surface water. The largest observed difference between the two scenarios (1.25 feet) was observed in the city of Oak Ridge North, while the smallest differences (about 0.2 feet) were observed in areas along the border of the SJRA service area. In areas not within the vicinity of the SJRA service area receiving treated surface water, there is no difference in total subsidence occurring between 2018-2070.

The final subsidence grids were resampled so that the cell sizes are identical to the cell size of topographic surfaces used by Michael Baker in the hydrologic and hydraulic models. In addition to the subsidence for 2070 for the two scenarios shown in **Figures 4-1 and 4-2**, two animations are included with this report that show the cumulative subsidence year by year from 2018 to 2070.

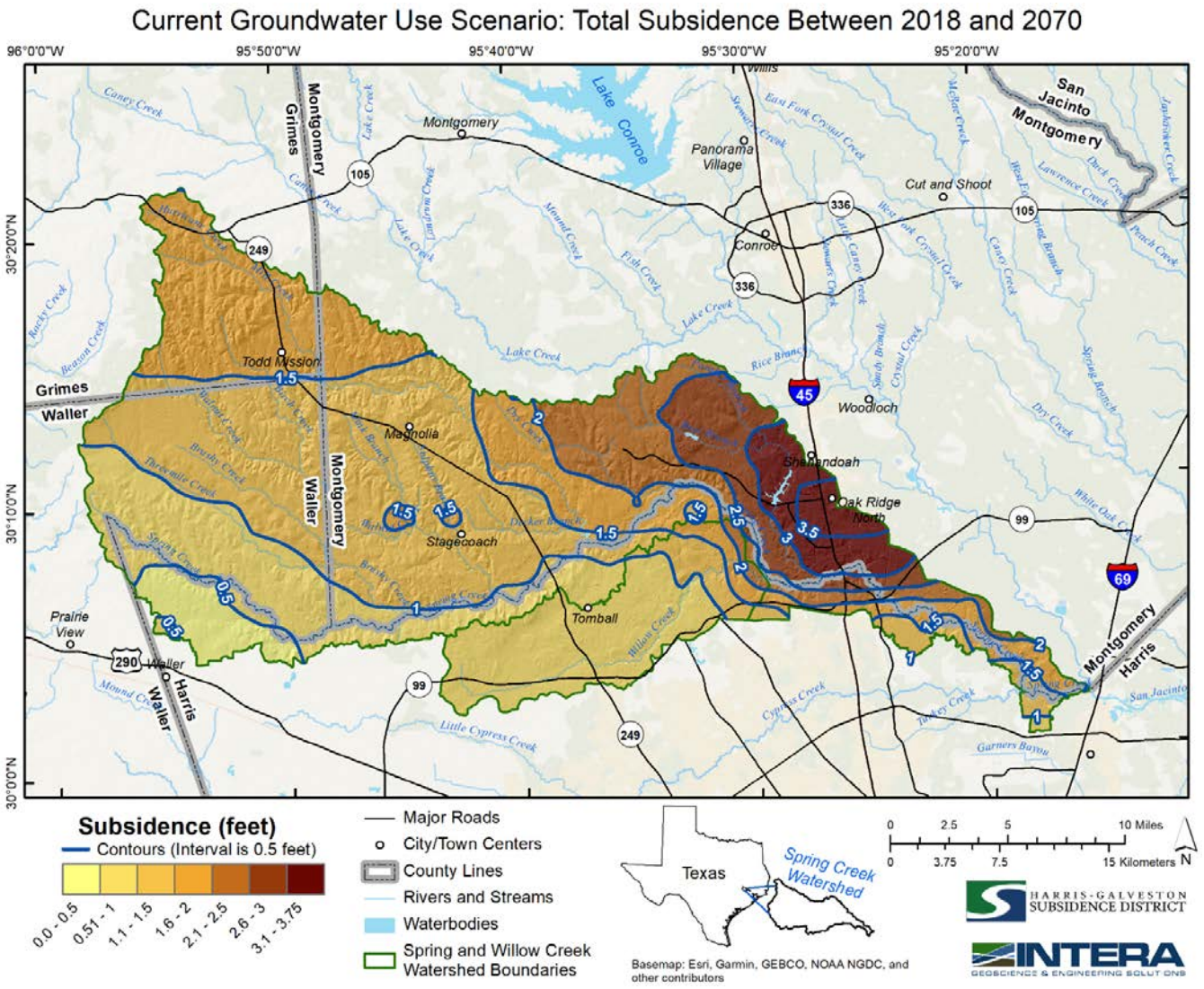

Figure 4-1 Total subsidence between 2018 and 2070 in the Current Groundwater Use (CGWU) scenario.

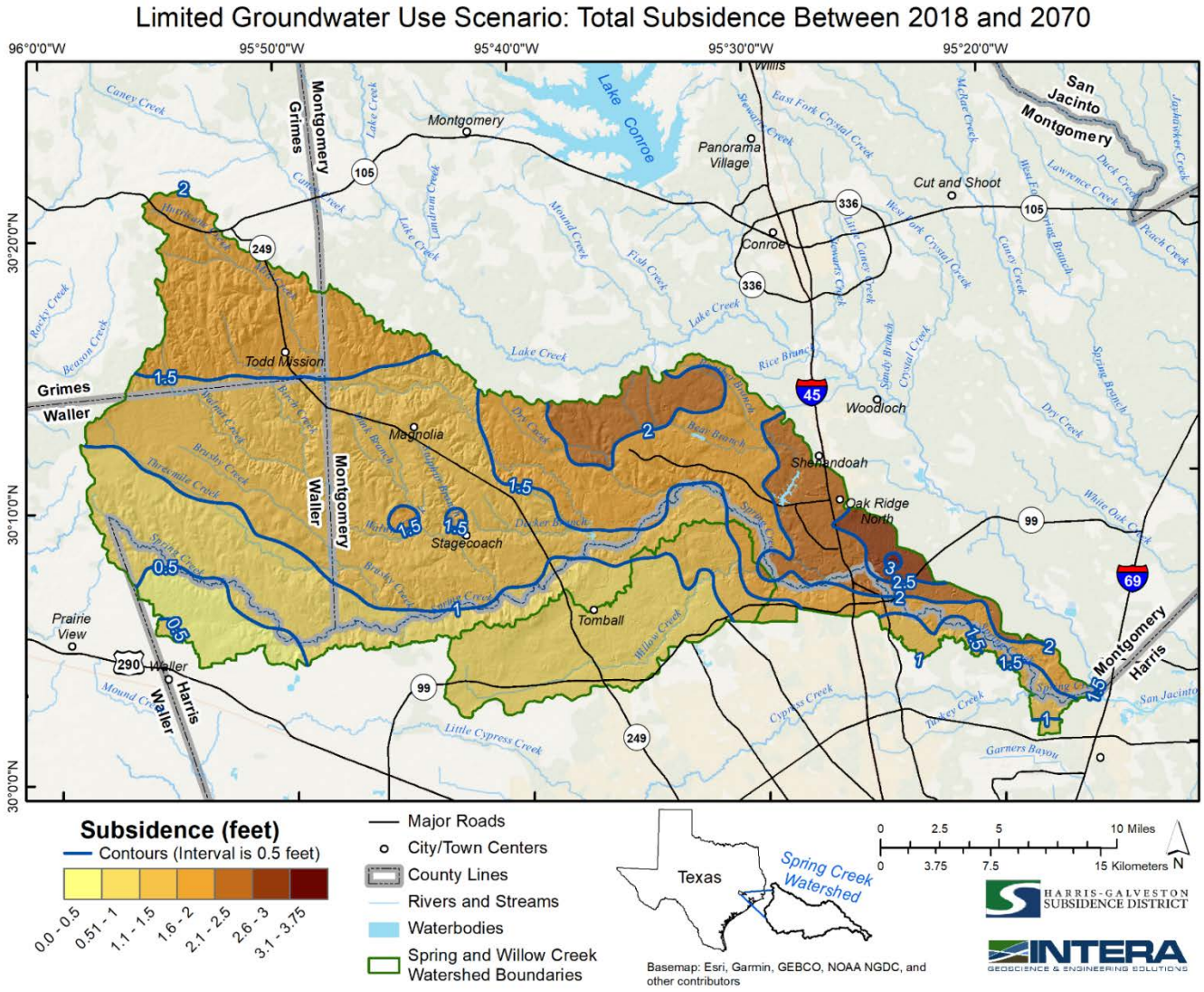

Figure 4-2 Total subsidence between 2018 and 2070 in the Limited Groundwater Use (LGWU) scenario.

5.0 REFERENCES

Kasmarek, Mark C. and Robinson, James L., 2004, Hydrogeology and Simulation of Ground Water Flow and Land-Surface Subsidence in the Northern Part of the Gulf Coast Aquifer System, Texas, U. S. Geological Survey Scientific Investigations Report 2004-5102, 103 pages.

Kasmarek, M.C. Hydrogeology and Simulation of Groundwater Flow and Land-Surface Subsidence in the Northern Part of the Gulf Coast Aquifer System, Texas, 1891–2009; Scientific Investigation Report 2012-5154; U.S. Geological Survey: Reston, VA, USA, 2013.

Morton, R. A. 1979. "Temporal and spatial variations in shoreline changes and their implications, examples from the Texas Gulf Coast." J. Sediment. Res. 49(4): 1101-1111. https://doi.org/10.1306/212F78BF-2B24-11D7-8648000102C1865D.

Paine, J. G. 1991. "Late Quaternary depositional units, sea level, and vertical movement along the central Texas coast (Doctoral dissertation)." University of Texas, Austin, TX. 256.

Qu, F.F., Lu, Z., Zhang, Q., Bawden, G.W., Kim, J.W., Zhao, C.Y., and Qu, W., 2015. Mapping ground deformation over Houston-Galveston, Texas using Multi-temporal InSAR, Remote Sensing of Environment, 169, 290-306.

Qu, F.F., Lu, Z., Kim, J.W., and Zheng, W.Y., 2019. Identify and monitor growth faulting using InSAR over northern Greater Houston region, Remote Sensing, 11, 1498; doi:10.3390/rs11121498.

Solt, Mike, and Michelle Sneed. Subsidence (2004-2009) in and near lakebeds of the Mojave River and Morongo groundwater basins, southwest Mojave Desert, California. No. 2014-5011. US Geological Survey, 2014.

Winker, C. D. 1979. "Late Pleistocene fluvial-deltaic deposition of the Texas coastal plain and shelf (M.A. thesis)." University of Texas at Austin, 187P.

Zhou, X., Wang, G., Wang, K., Liu, H., Lyu, H., and Turco, M., 2021. Rates of Natural Subsidence and Submergence Along the Texas Coast Derived from GPS and Tide Gauge Measurements (1904-2020), Journal of Surveying Engineering (*in press*).

This page is intentionally left blank.

APPENDIX A:
FIGURES DEVELOPED FOR SELECTED GPS STATIONS

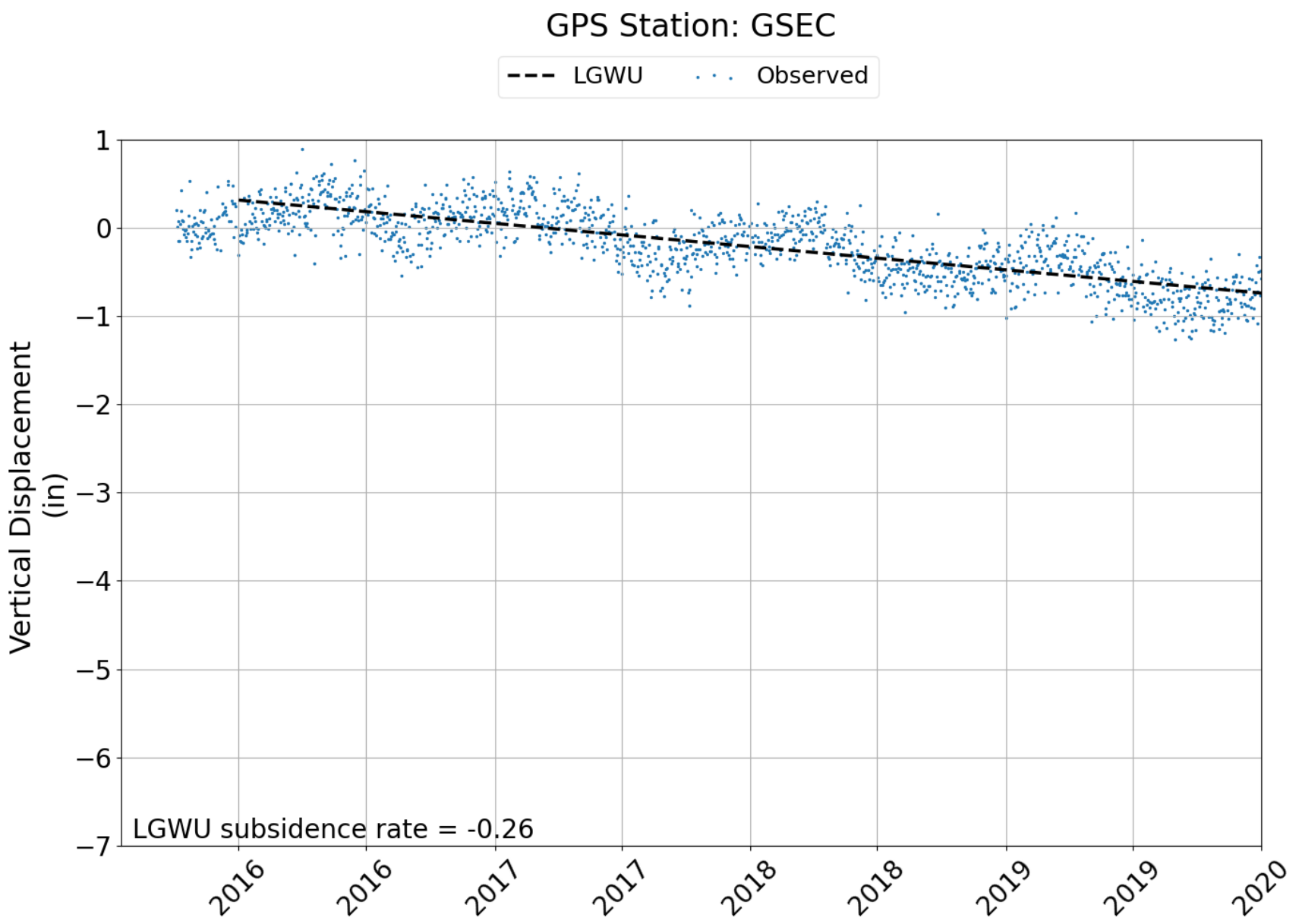
GPS Station: GSEC
LGWU
Observed
Vertical Displacement (in)
1
0
−1
−2
−3
−4
−5
−6
−7
LGWU subsidence rate = -0.26
2016
2016
2017
2017
2018
2018
2019
2019
2020

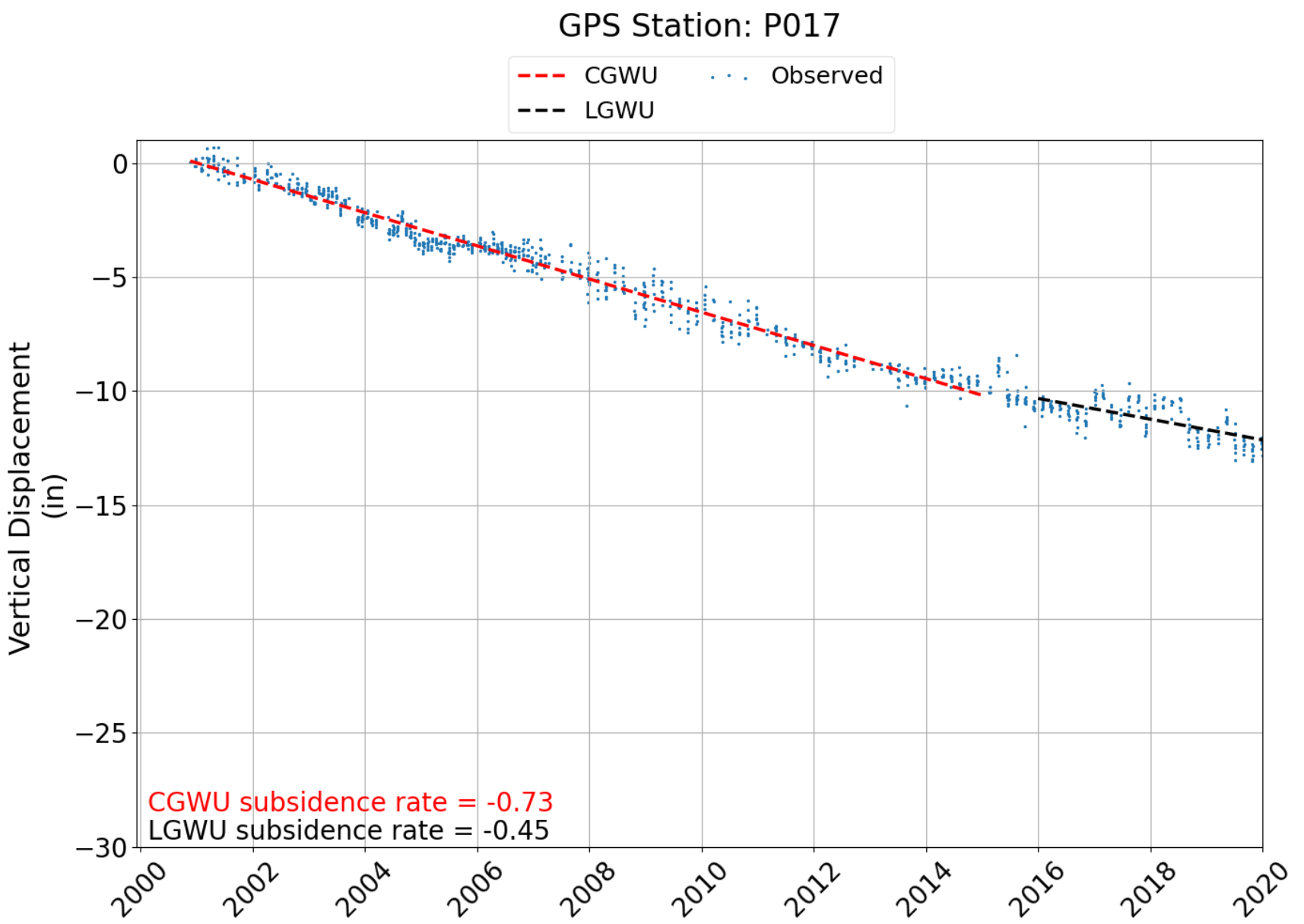
GPS Station: P017
CGWU
LGWU
Observed
Vertical Displacement (in)
0
−5
−10
−15
−20
−25
−30
2000
2002
2004
2006
2008
2010
2012
2014
2016
2018
2020
CGWU subsidence rate = -0.73
LGWU subsidence rate = -0.45

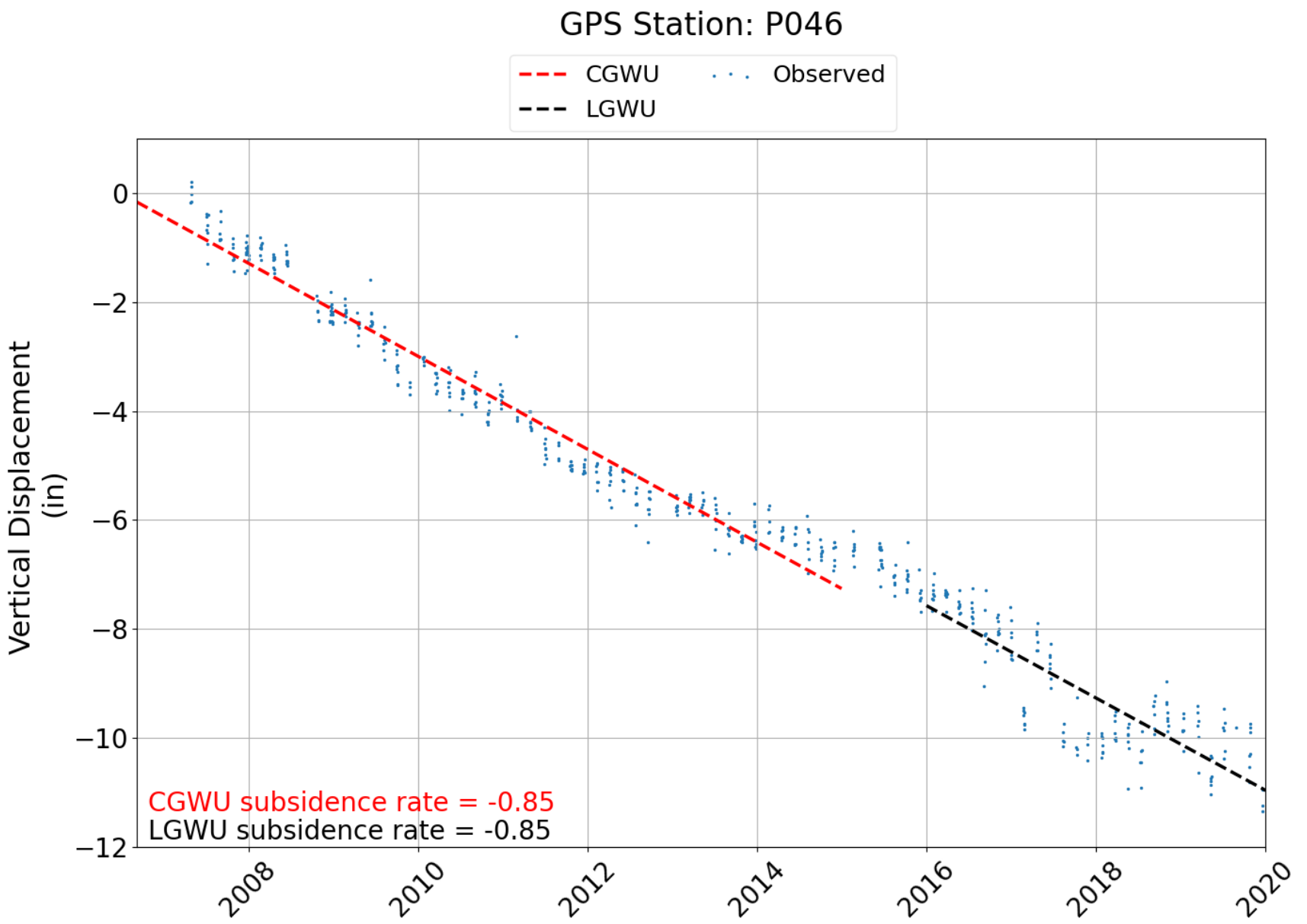
GPS Station: P046
CGWU
LGWU
Observed
Vertical Displacement (in)
0
−2
−4
−6
−8
−10
−12
2008
2010
2012
2014
2016
2018
2020
CGWU subsidence rate = -0.85
LGWU subsidence rate = -0.85

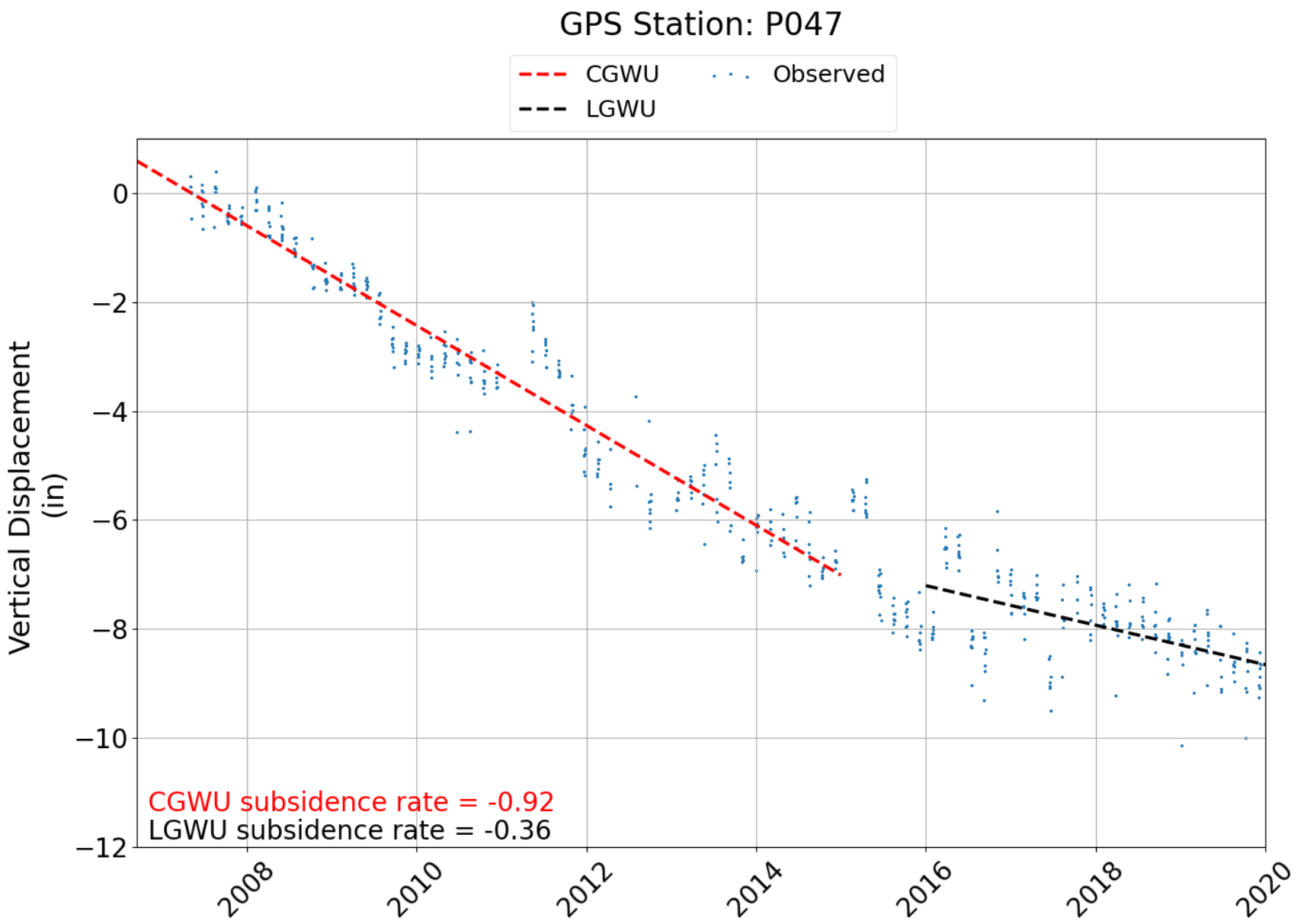
GPS Station: P047
CGWU
LGWU
Observed
Vertical Displacement (in)
0
−2
−4
−6
−8
−10
−12
2008
2010
2012
2014
2016
2018
2020
CGWU subsidence rate = -0.92
LGWU subsidence rate = -0.36

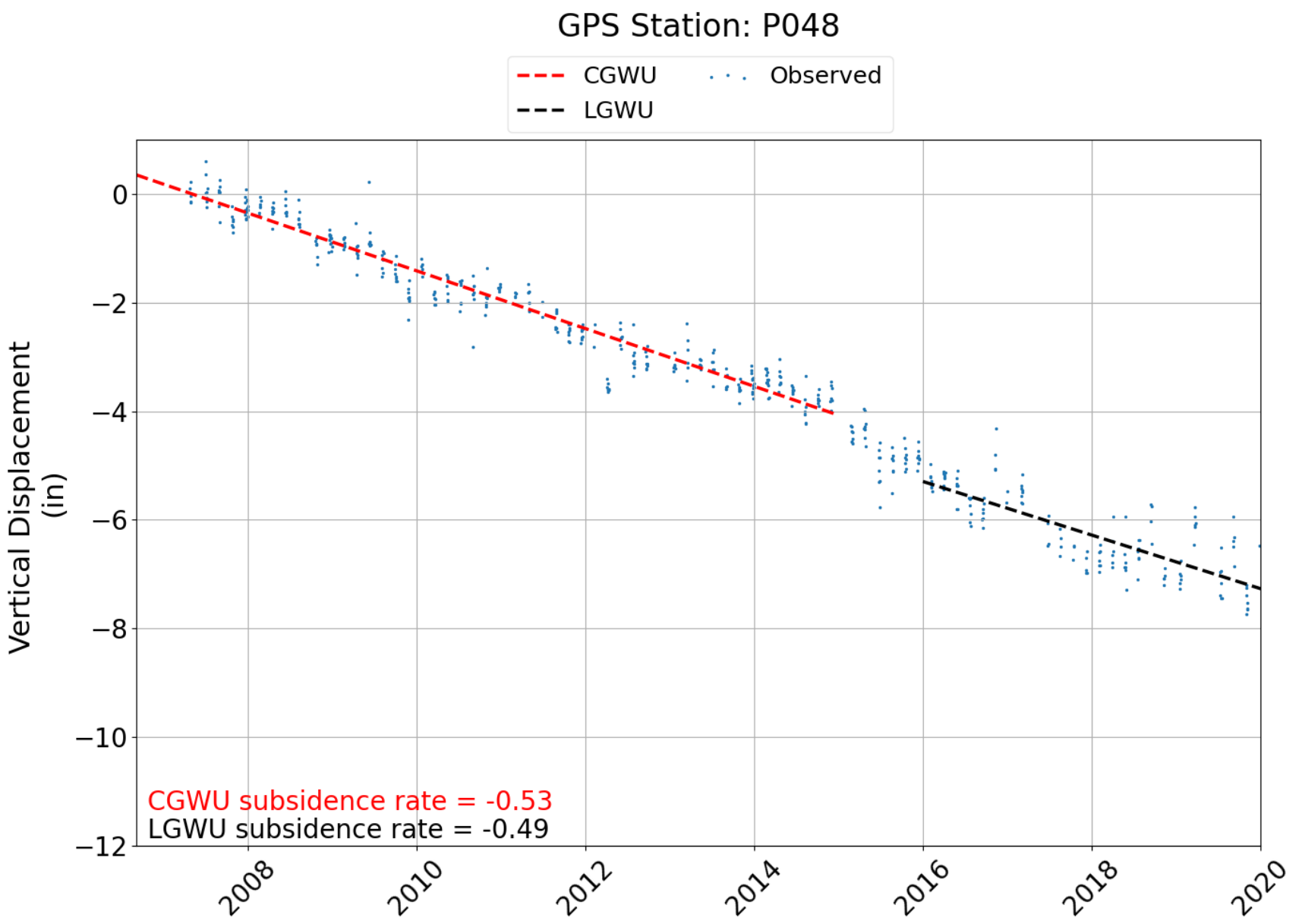
GPS Station: P048
CGWU
LGWU
Observed
Vertical Displacement (in)
0
−2
−4
−6
−8
−10
−12
2008
2010
2012
2014
2016
2018
2020
CGWU subsidence rate = -0.53
LGWU subsidence rate = -0.49

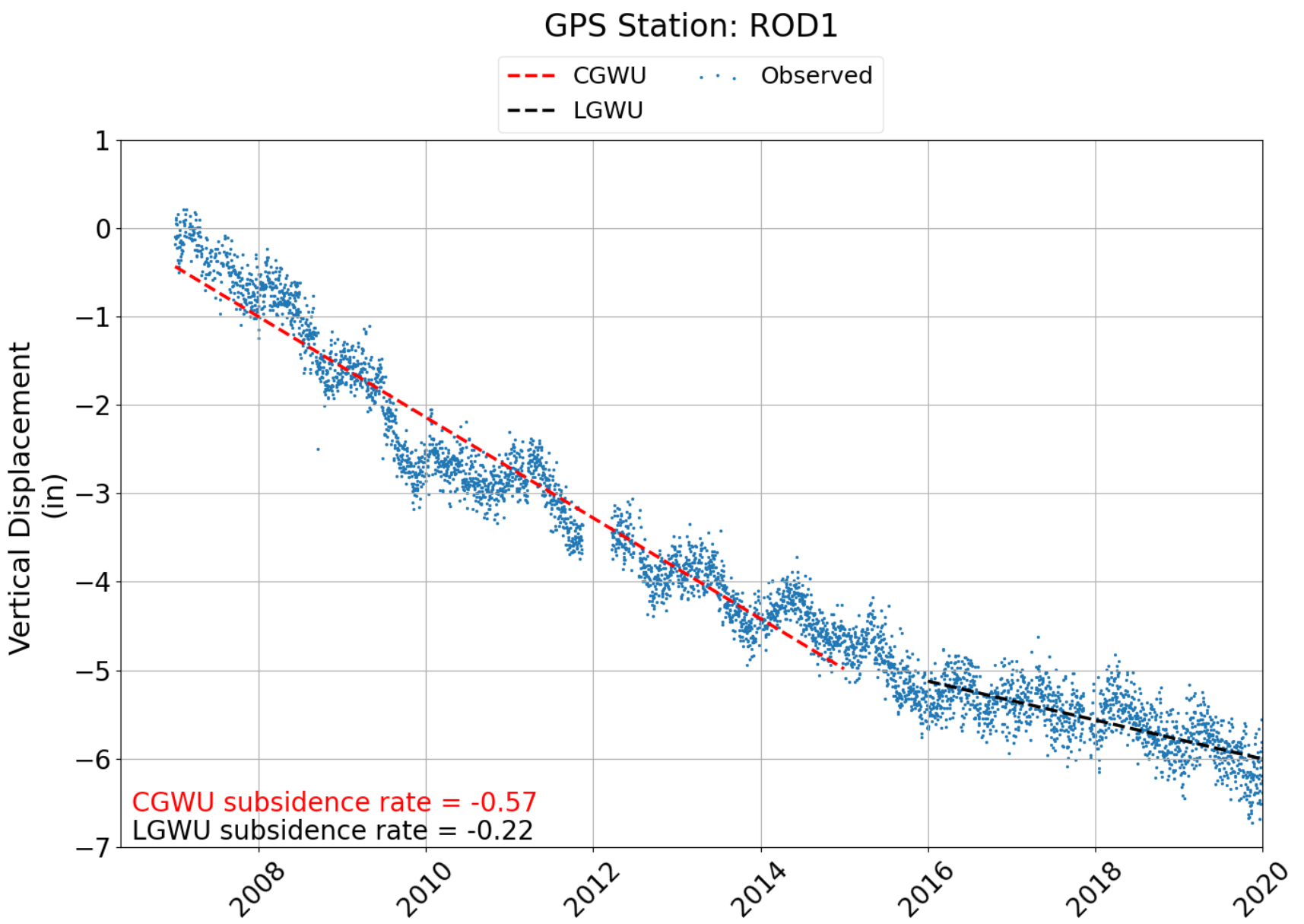
GPS Station: ROD1
CGWU
LGWU
Observed
Vertical Displacement (in)
1
0
−1
−2
−3
−4
−5
−6
−7
2008
2010
2012
2014
2016
2018
2020
CGWU subsidence rate = -0.57
LGWU subsidence rate = -0.22

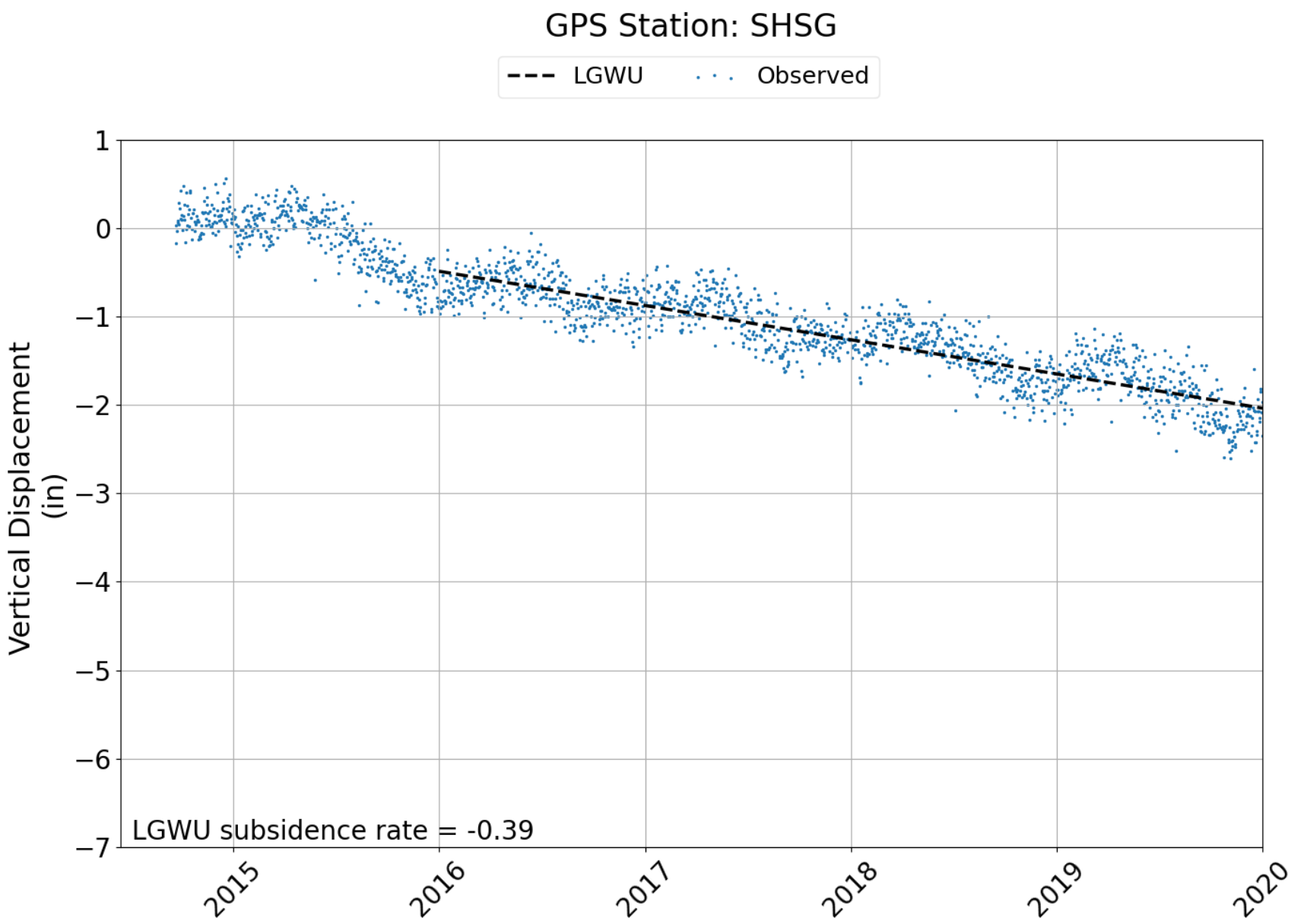
GPS Station: SHSG
LGWU
Observed
Vertical Displacement (in)
1
0
−1
−2
−3
−4
−5
−6
−7
LGWU subsidence rate = -0.39
2015
2016
2017
2018
2019
2020

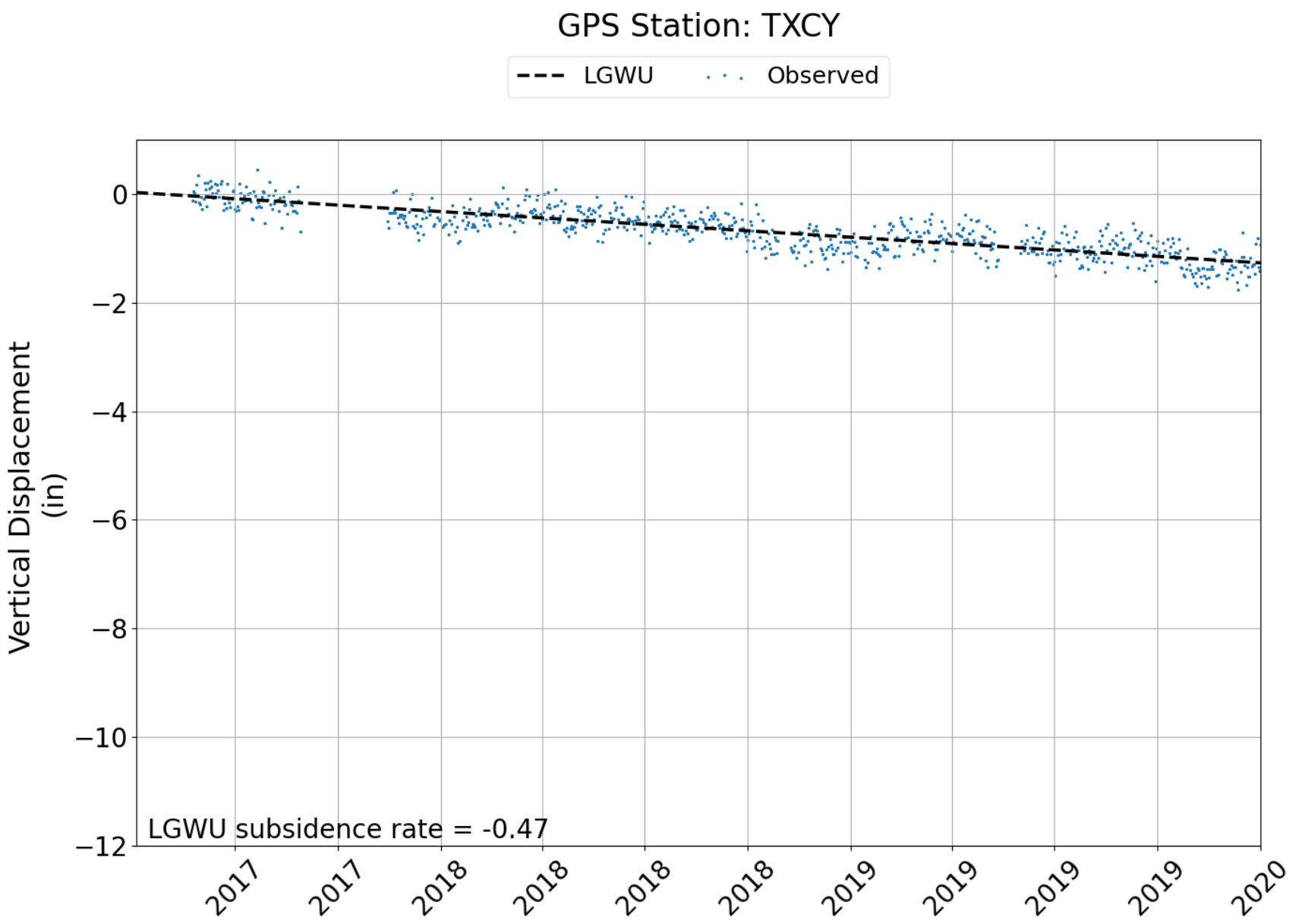
GPS Station: TXCY
LGWU
Observed
Vertical Displacement (in)
0
−2
−4
−6
−8
−10
−12
LGWU subsidence rate = -0.47
2017
2017
2018
2018
2018
2018
2019
2019
2019
2019
2020

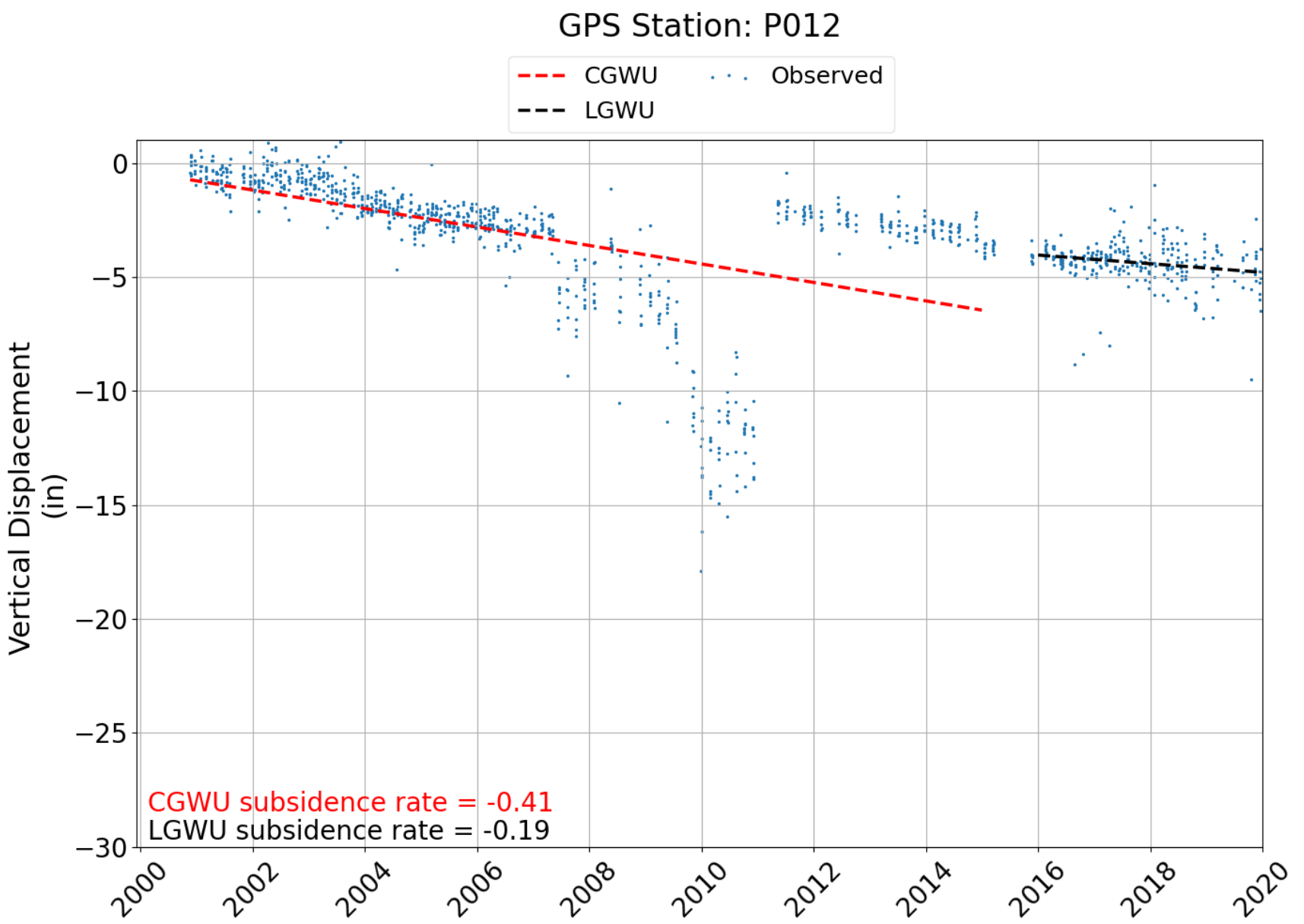
GPS Station: P012
CGWU
LGWU
Observed
Vertical Displacement (in)
0
−5
−10
−15
−20
−25
−30
2000
2002
2004
2006
2008
2010
2012
2014
2016
2018
2020
CGWU subsidence rate = -0.41
LGWU subsidence rate = -0.19

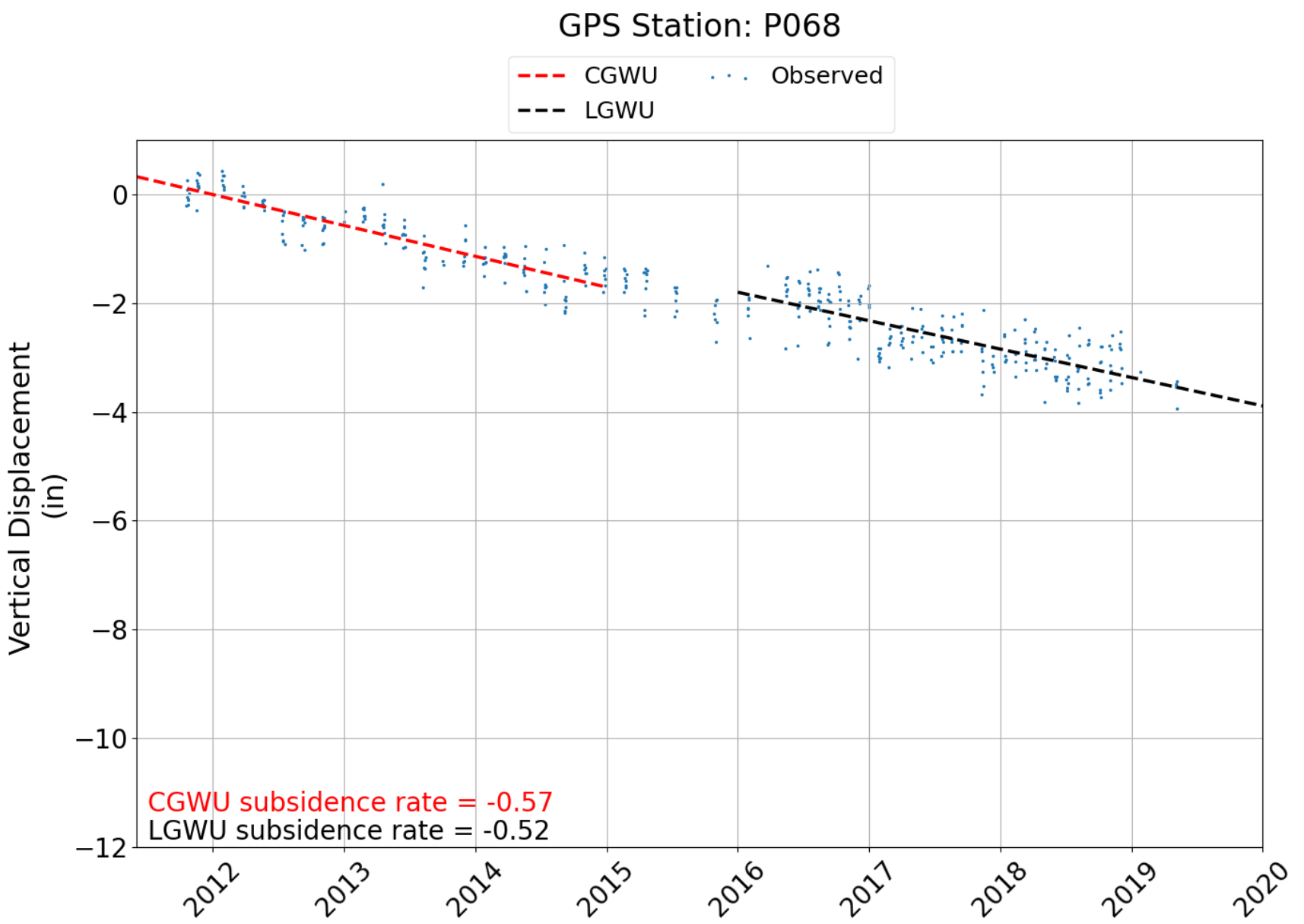
GPS Station: P068
CGWU
LGWU
Observed
Vertical Displacement (in)
0
−2
−4
−6
−8
−10
−12
2012
2013
2014
2015
2016
2017
2018
2019
2020
CGWU subsidence rate = -0.57
LGWU subsidence rate = -0.52

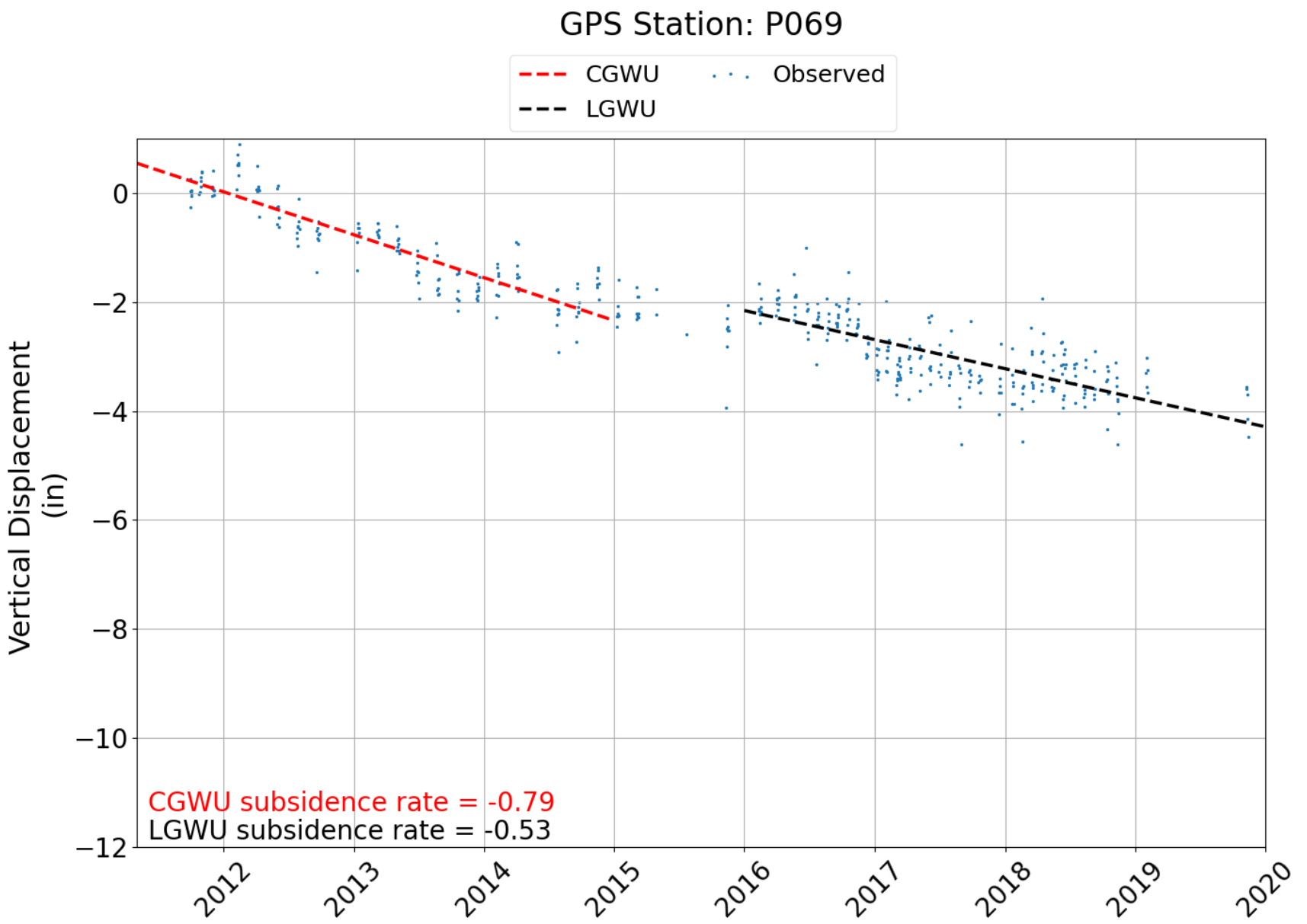
GPS Station: P069
CGWU
LGWU
Observed
Vertical Displacement (in)
0
−2
−4
−6
−8
−10
−12
2012
2013
2014
2015
2016
2017
2018
2019
2020
CGWU subsidence rate = -0.79
LGWU subsidence rate = -0.53

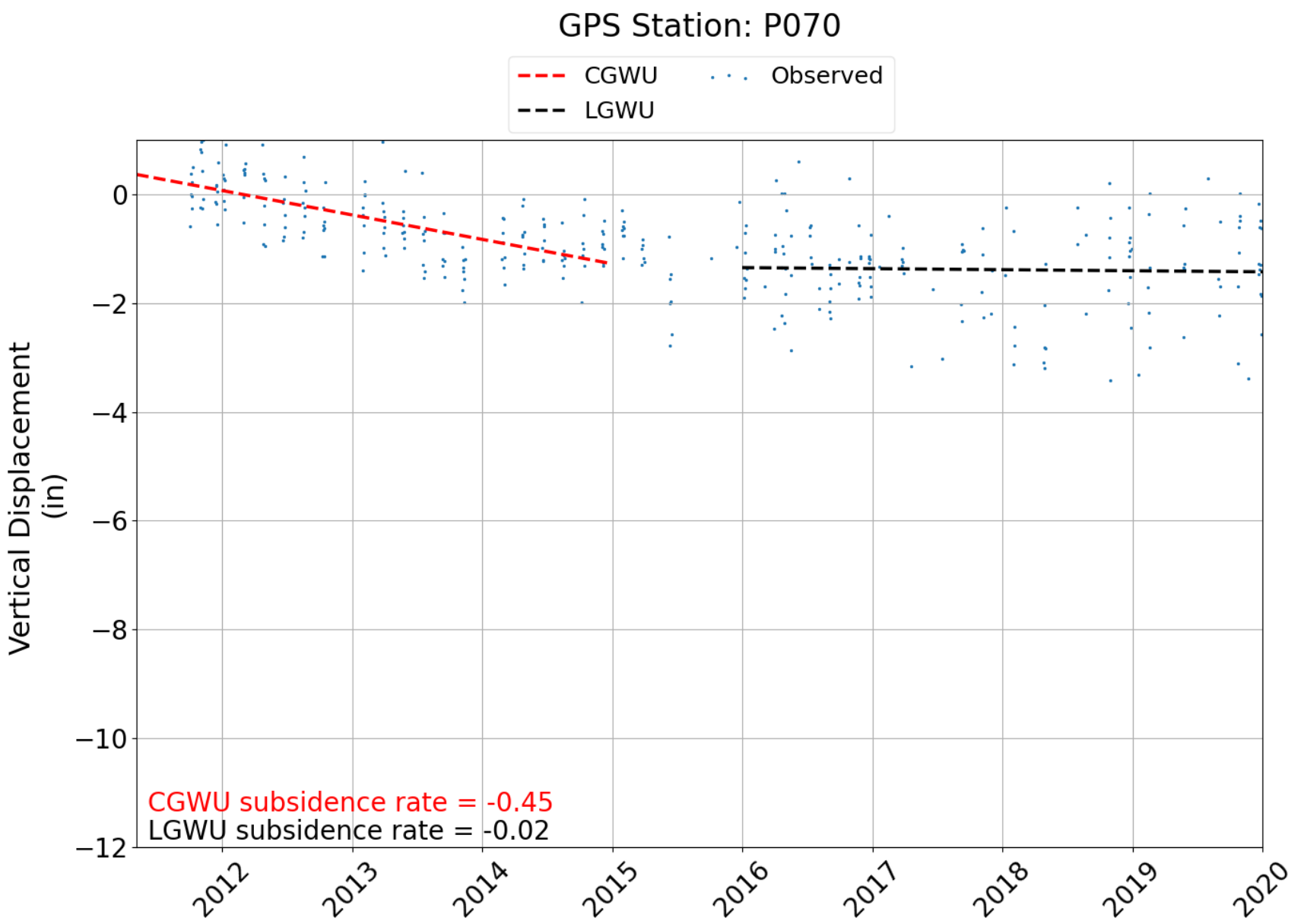
GPS Station: P070
CGWU
LGWU
Observed
Vertical Displacement (in)
0
−2
−4
−6
−8
−10
−12
2012
2013
2014
2015
2016
2017
2018
2019
2020
CGWU subsidence rate = -0.45
LGWU subsidence rate = -0.02

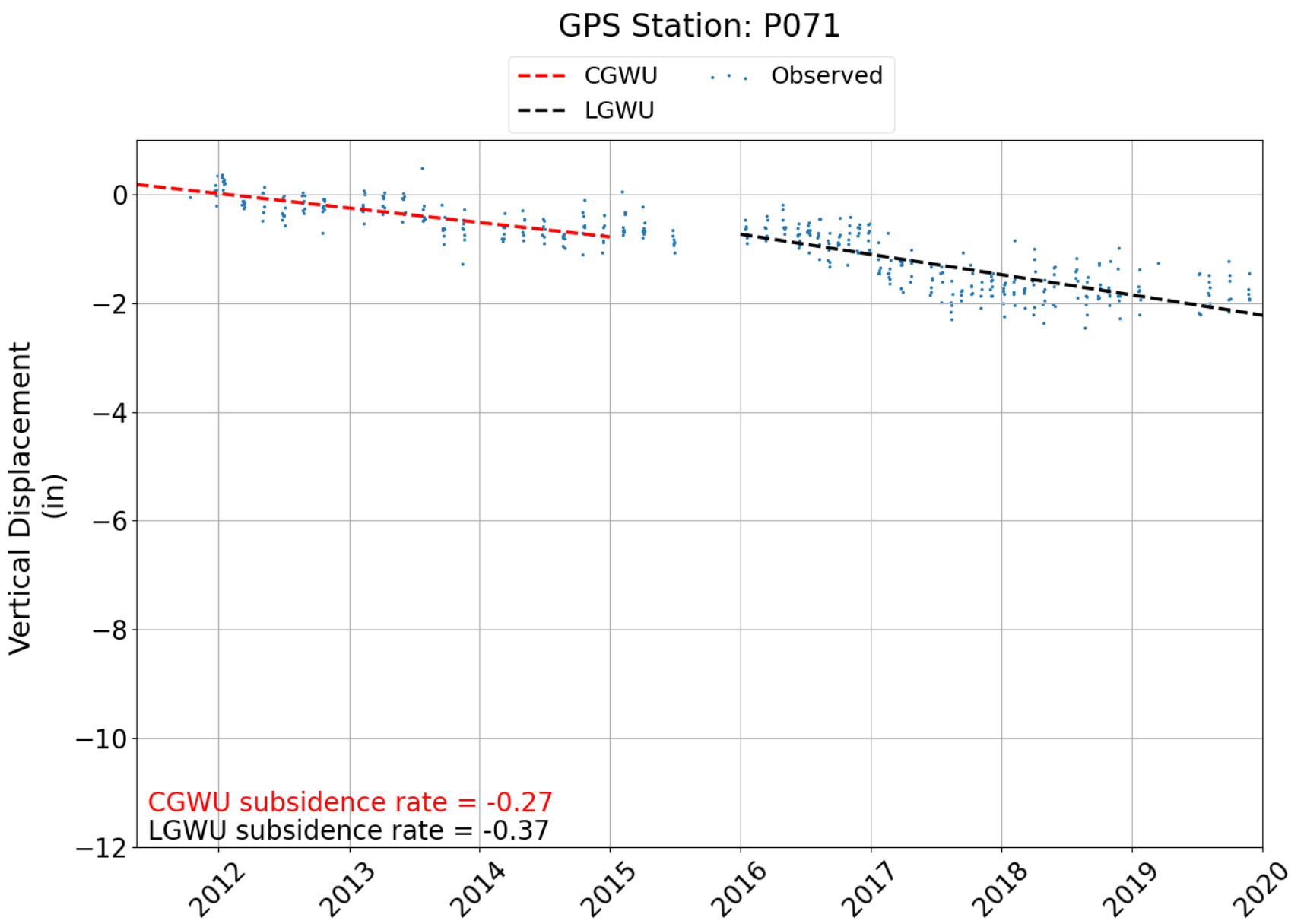
GPS Station: P071
CGWU
LGWU
Observed
Vertical Displacement (in)
0
−2
−4
−6
−8
−10
−12
2012
2013
2014
2015
2016
2017
2018
2019
2020
CGWU subsidence rate = -0.27
LGWU subsidence rate = -0.37

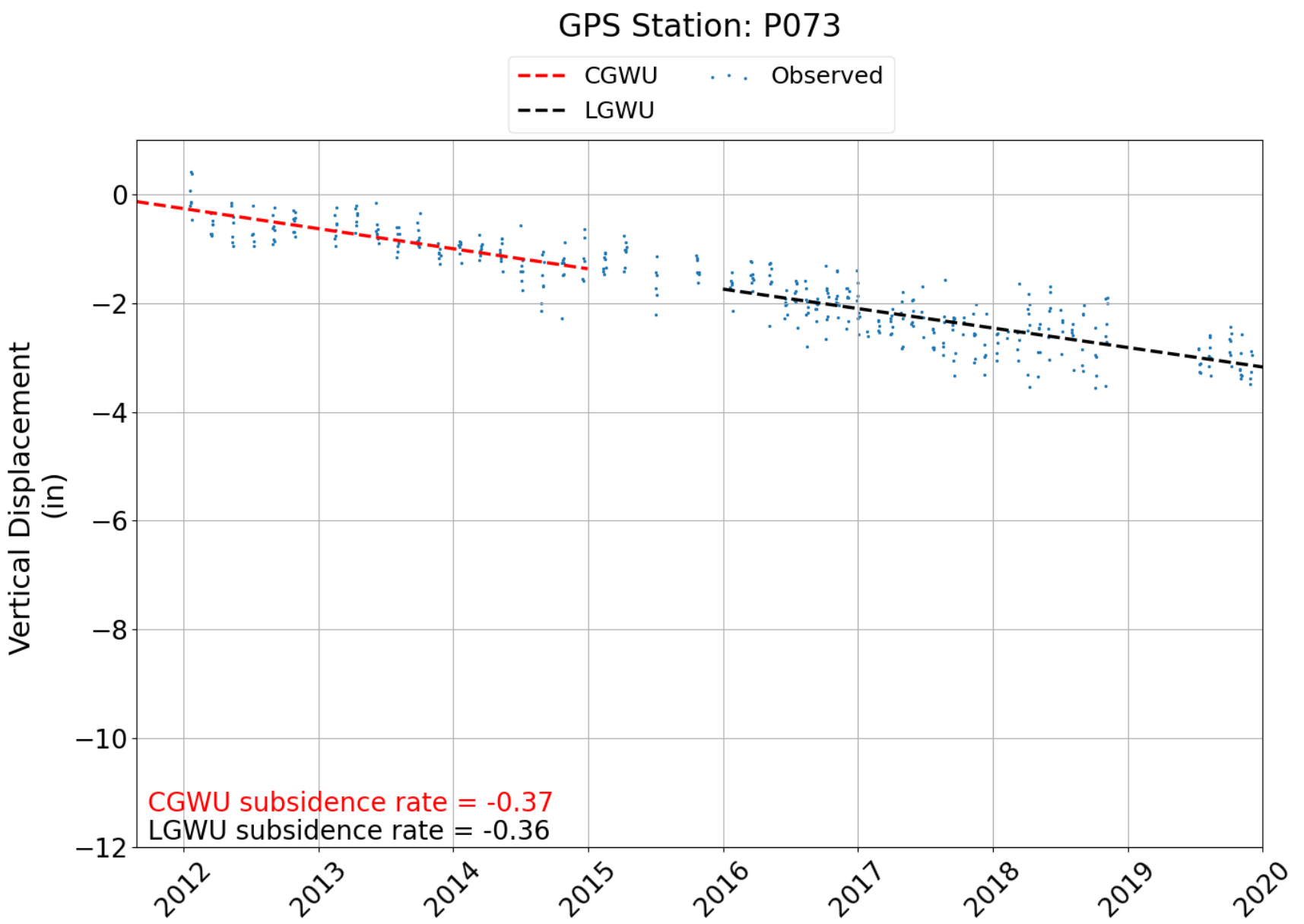
GPS Station: P073
CGWU
LGWU
Observed
Vertical Displacement (in)
0
−2
−4
−6
−8
−10
−12
2012
2013
2014
2015
2016
2017
2018
2019
2020
CGWU subsidence rate = -0.37
LGWU subsidence rate = -0.36

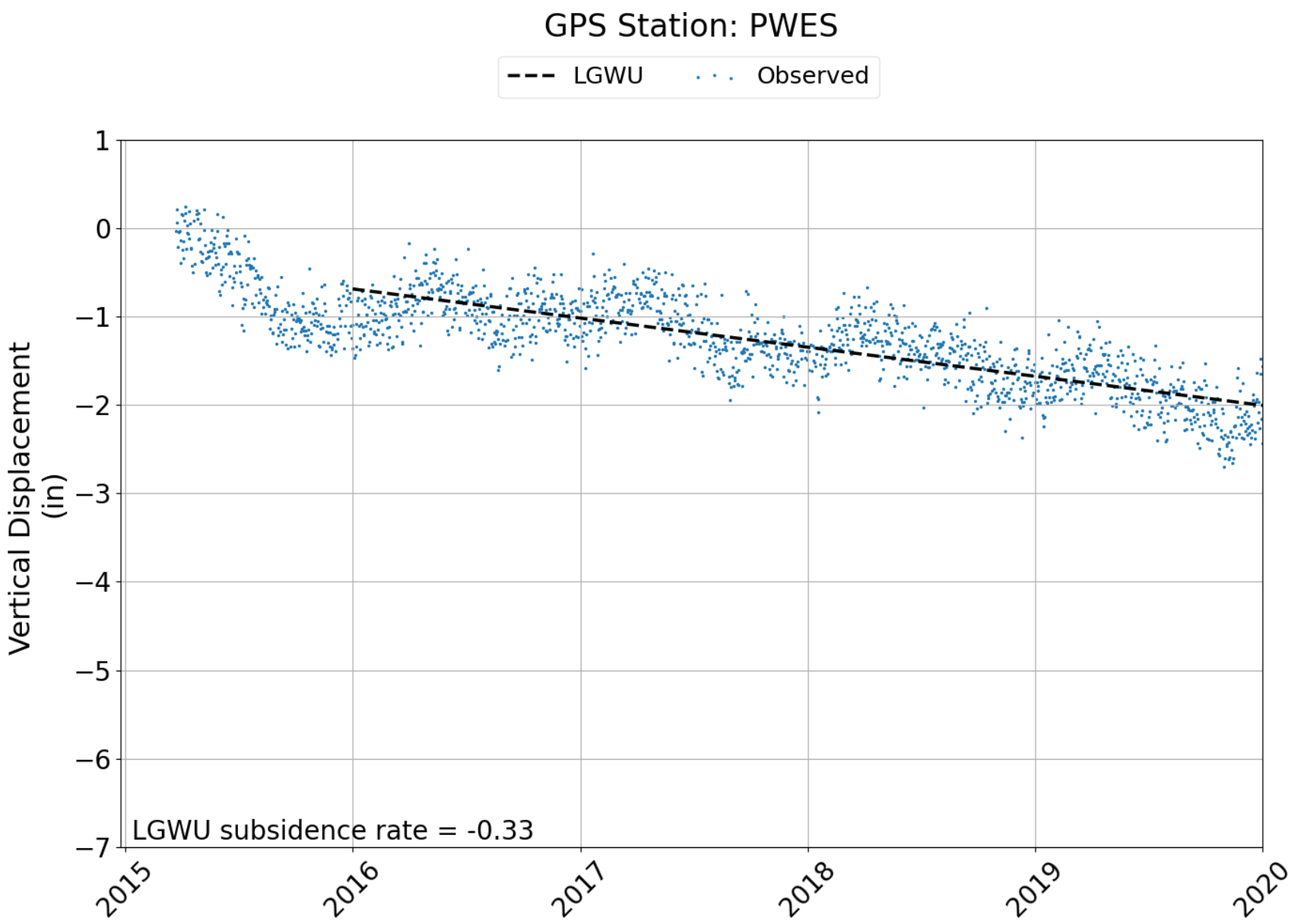
GPS Station: PWES
LGWU
Observed
Vertical Displacement (in)
1
0
−1
−2
−3
−4
−5
−6
−7
LGWU subsidence rate = -0.33
2015
2016
2017
2018
2019
2020

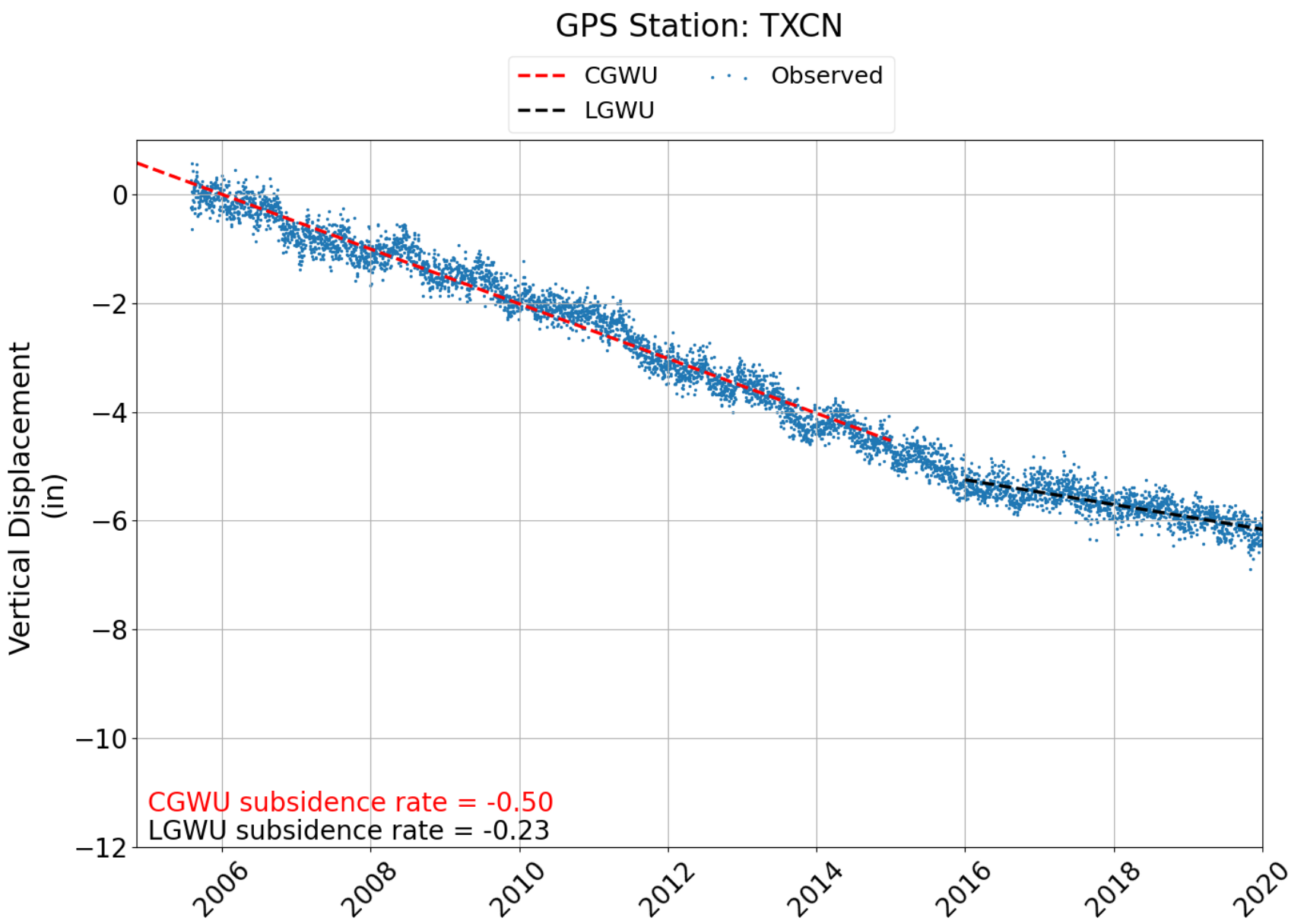
GPS Station: TXCN
CGWU
LGWU
Observed
Vertical Displacement (in)
0
−2
−4
−6
−8
−10
−12
2006
2008
2010
2012
2014
2016
2018
2020
CGWU subsidence rate = -0.50
LGWU subsidence rate = -0.23

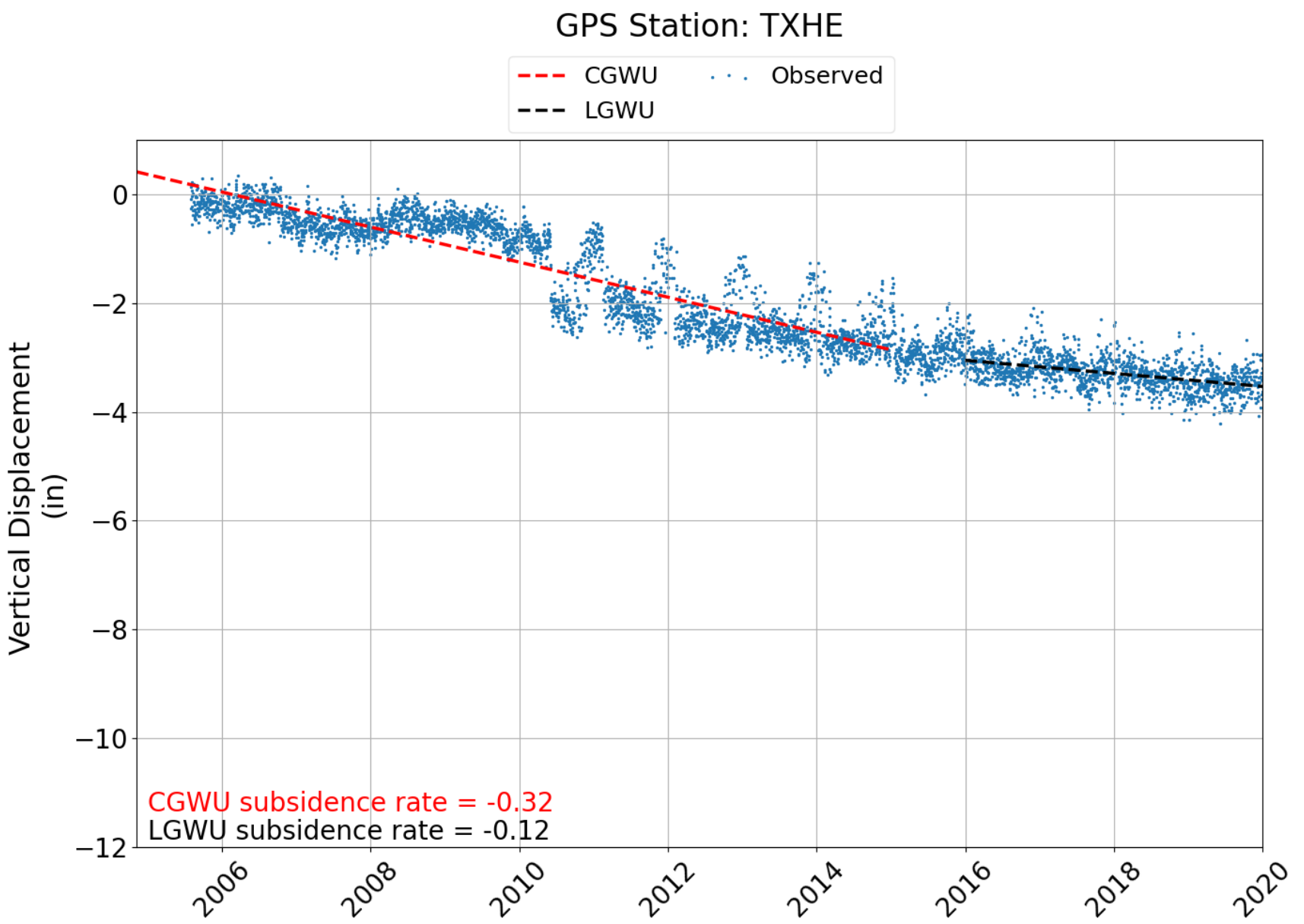
GPS Station: TXHE
CGWU
LGWU
Observed
Vertical Displacement (in)
0
−2
−4
−6
−8
−10
−12
2006
2008
2010
2012
2014
2016
2018
2020
CGWU subsidence rate = -0.32
LGWU subsidence rate = -0.12

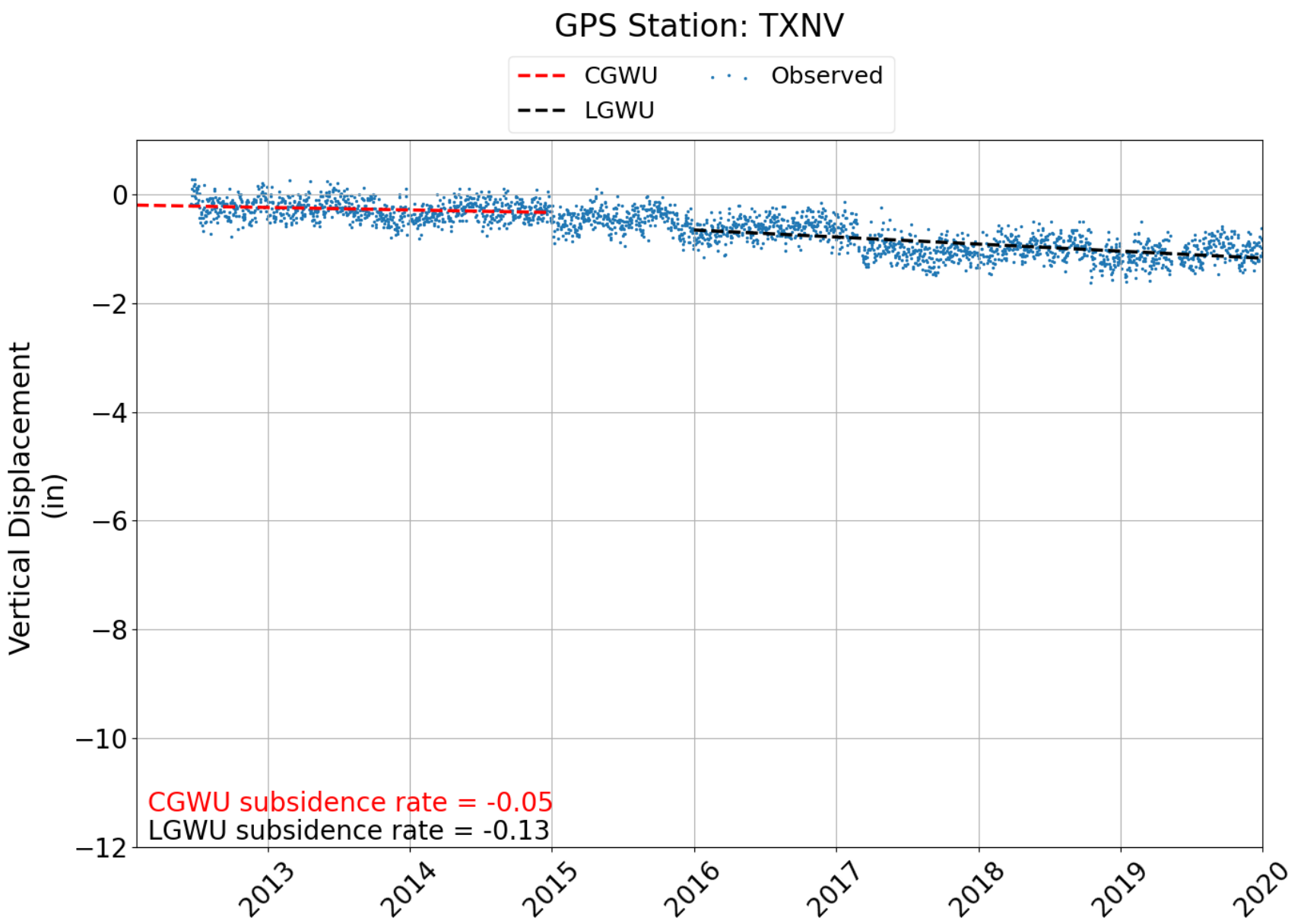
GPS Station: TXNV
CGWU
LGWU
Observed
Vertical Displacement (in)
0
−2
−4
−6
−8
−10
−12
2013
2014
2015
2016
2017
2018
2019
2020
CGWU subsidence rate = -0.05
LGWU subsidence rate = -0.13

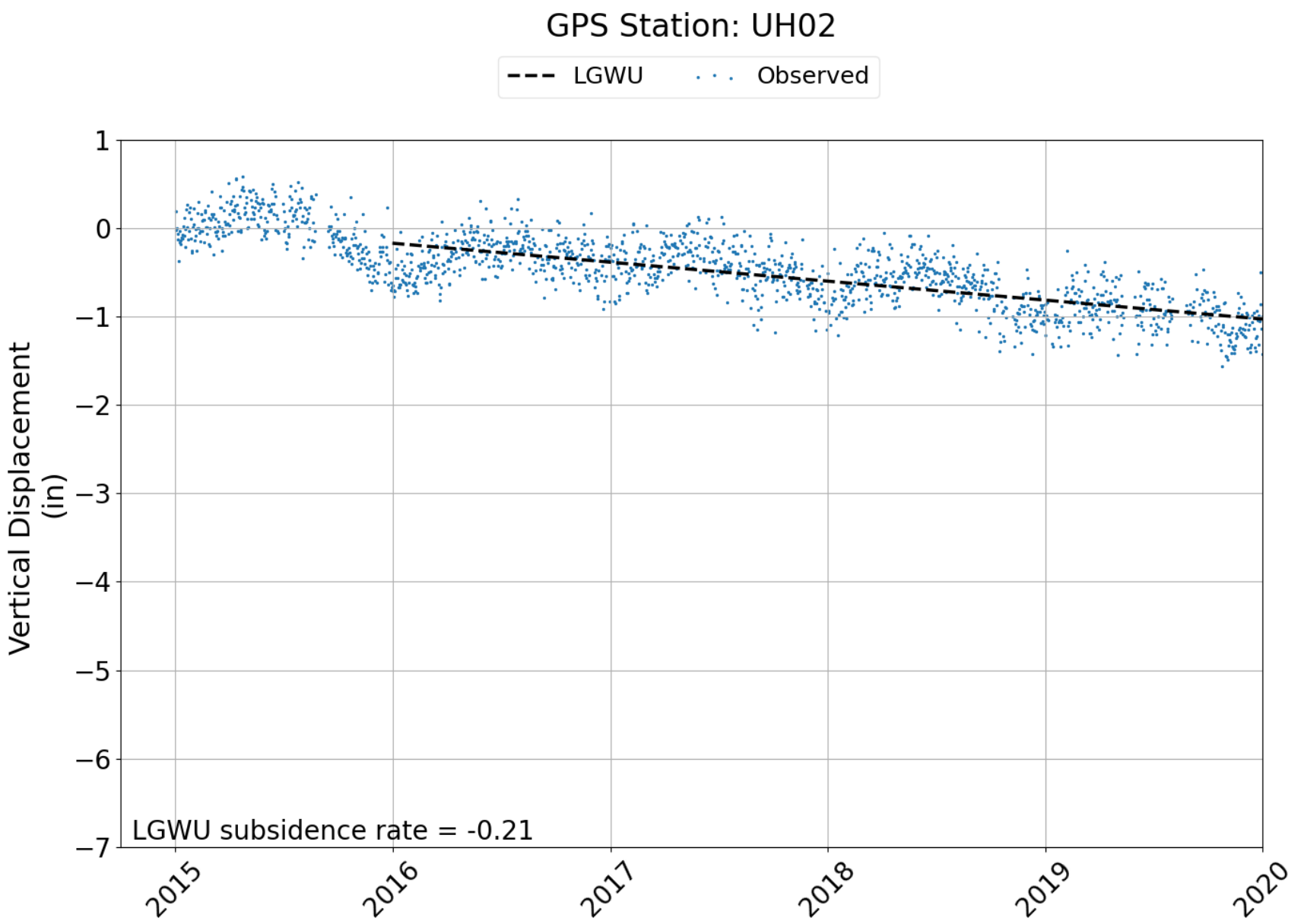
GPS Station: UH02
LGWU
Observed
Vertical Displacement (in)
1
0
−1
−2
−3
−4
−5
−6
−7
LGWU subsidence rate = -0.21
2015
2016
2017
2018
2019
2020

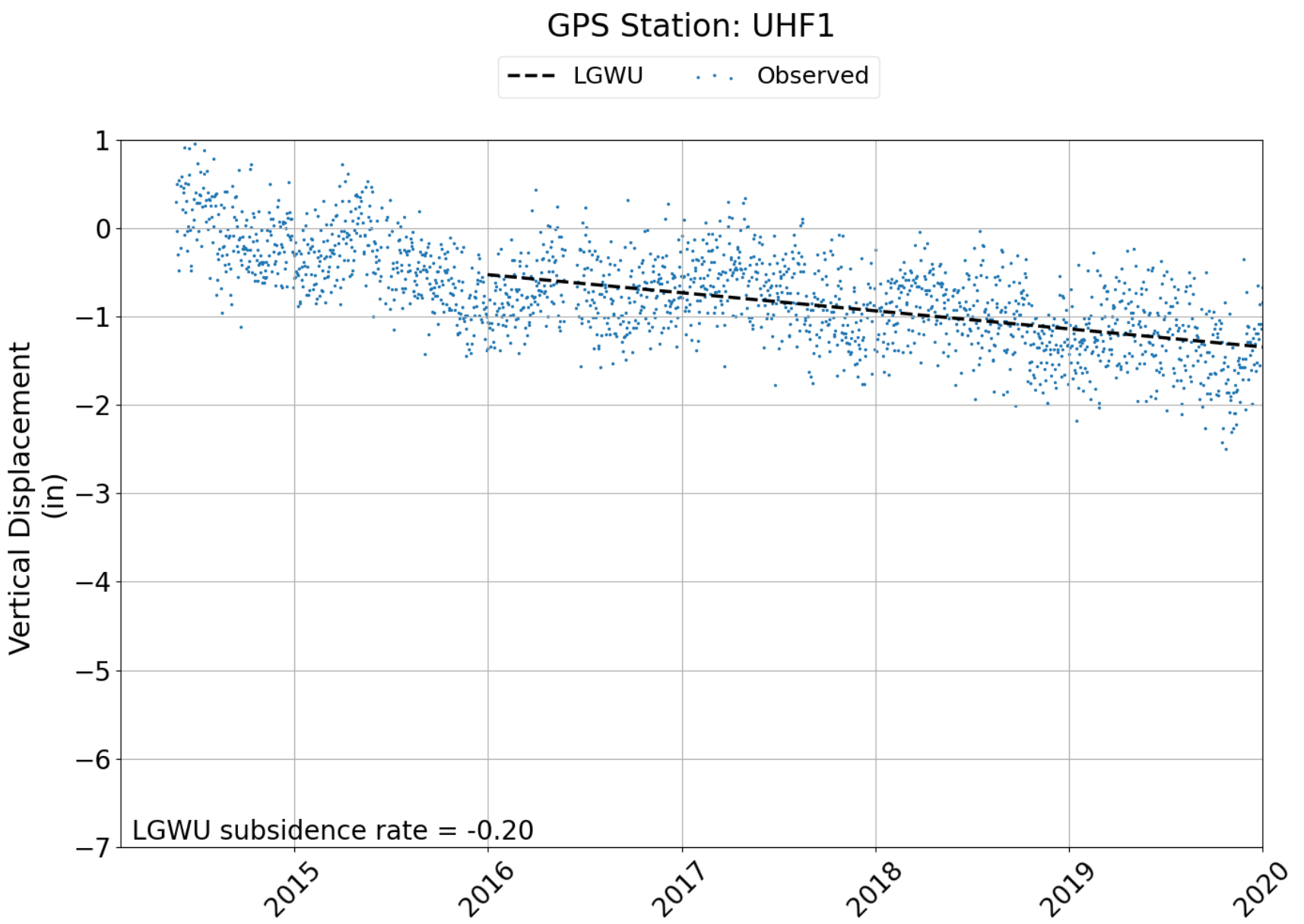
GPS Station: UHF1
LGWU
Observed
Vertical Displacement (in)
1
0
−1
−2
−3
−4
−5
−6
−7
LGWU subsidence rate = -0.20
2015
2016
2017
2018
2019
2020

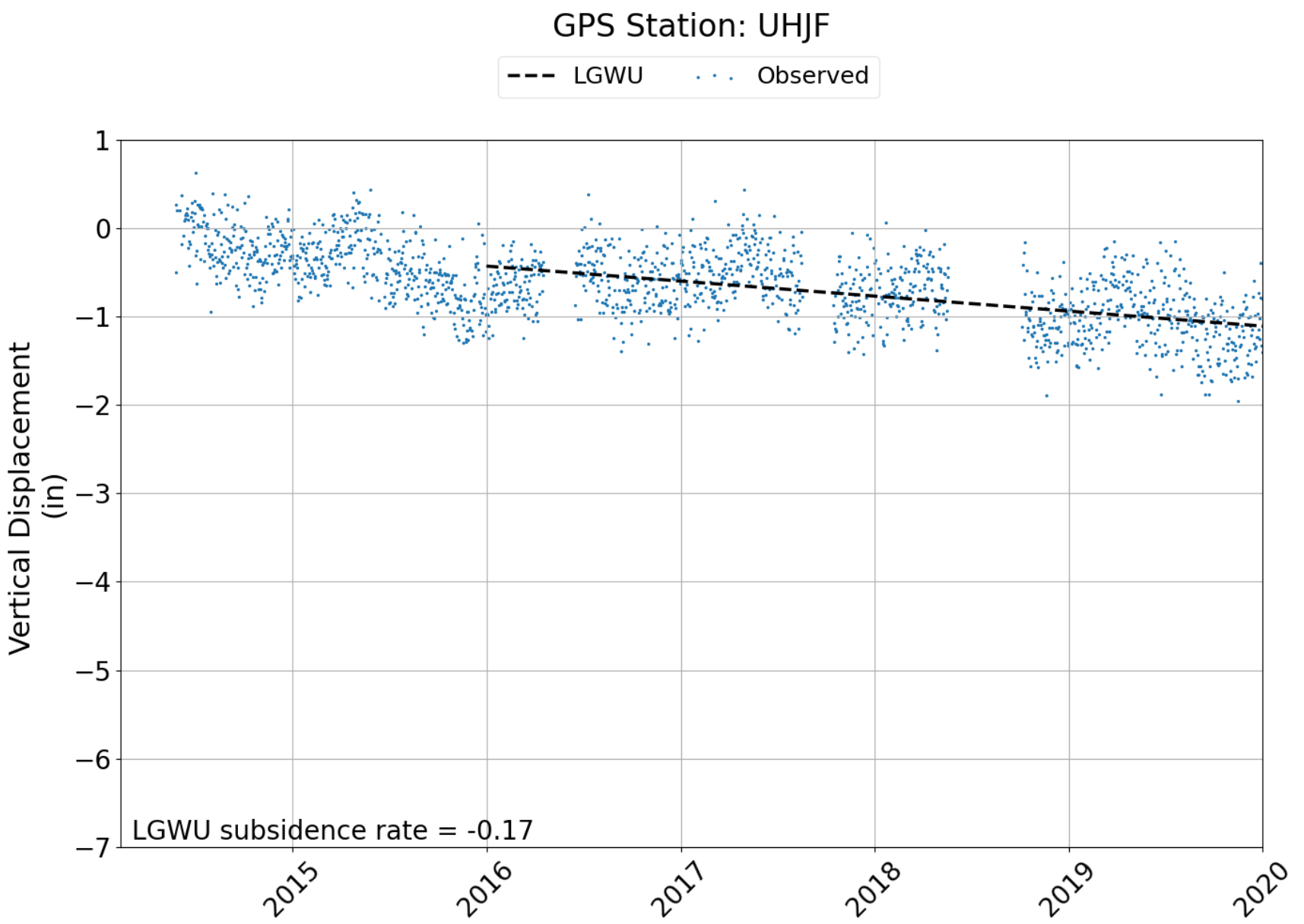
GPS Station: UHJF
LGWU
Observed
Vertical Displacement (in)
1
0
−1
−2
−3
−4
−5
−6
−7
LGWU subsidence rate = -0.17
2015
2016
2017
2018
2019
2020

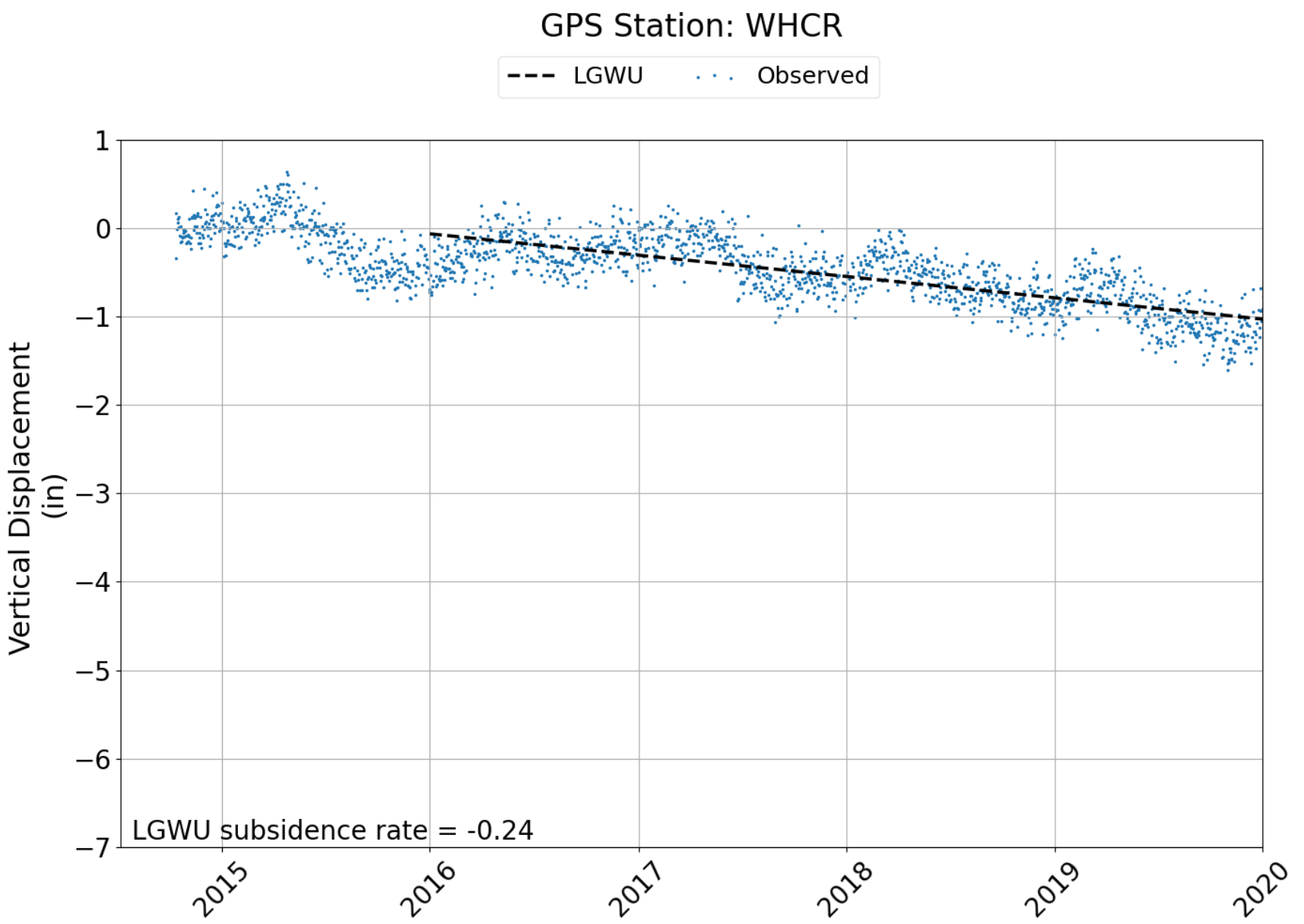
GPS Station: WHCR
LGWU
Observed
Vertical Displacement (in)
1
0
−1
−2
−3
−4
−5
−6
−7
LGWU subsidence rate = -0.24
2015
2016
2017
2018
2019
2020

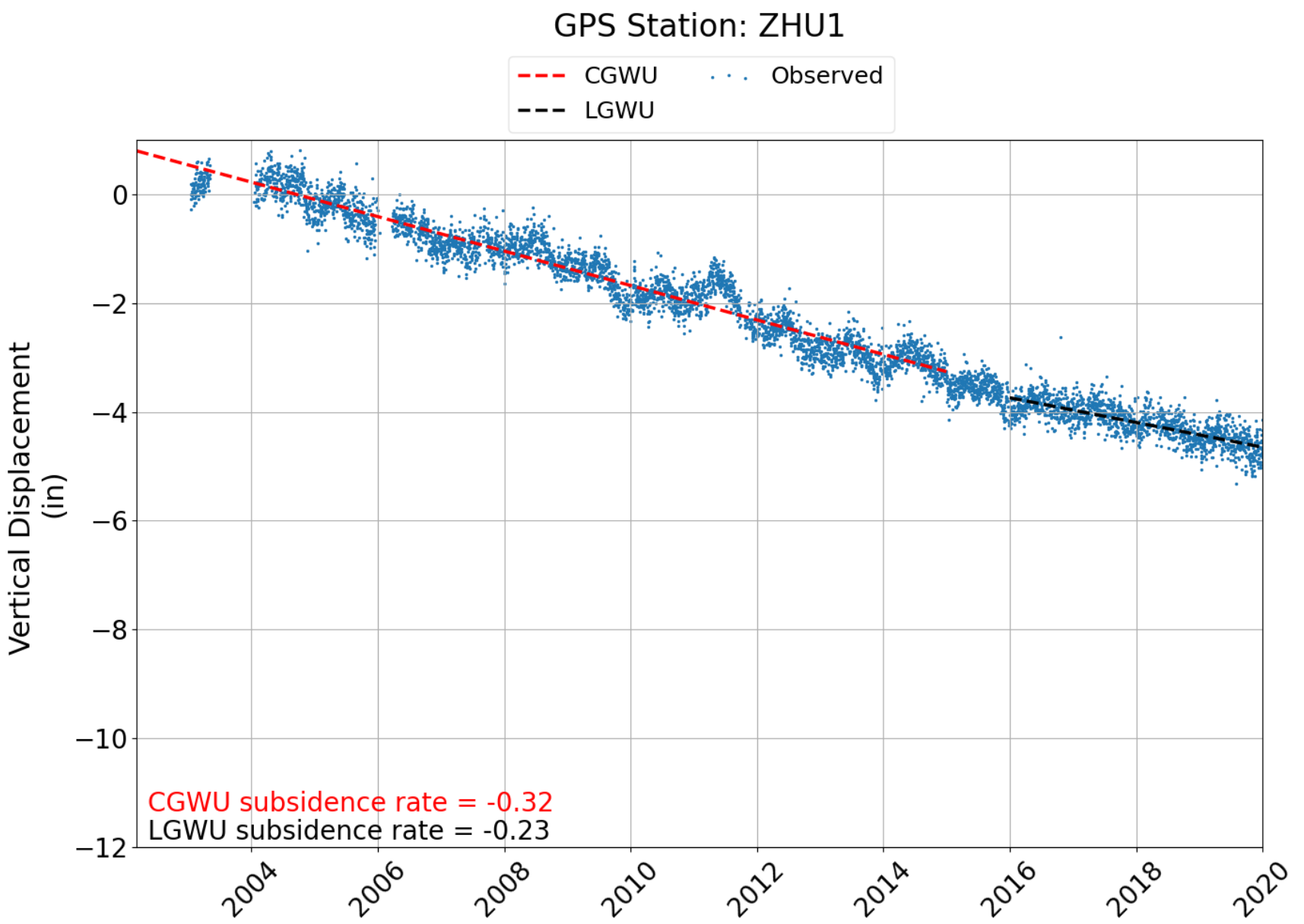
GPS Station: ZHU1
CGWU
LGWU
Observed
Vertical Displacement (in)
0
−2
−4
−6
−8
−10
−12
2004
2006
2008
2010
2012
2014
2016
2018
2020
CGWU subsidence rate = -0.32
LGWU subsidence rate = -0.23